

Use Authorization

In presenting this dissertation in partial fulfillment of the requirements for an advanced degree at Idaho State University, I agree that the Library shall make it freely available for inspection. I further state that permission to download and/or print my dissertation for scholarly purposes may be granted by the Dean of the Graduate School, Dean of my academic division, or by the University Librarian. It is understood that any copying or publication of this dissertation for financial gain shall not be allowed without my written permission.

Signature _____

Date _____

DEVELOPMENT AND APPLICATION OF AN AMERICIUM-DTPA
BIOKINETIC MODEL

by

Mason Mark Jausi

A thesis

submitted in partial fulfillment

of the requirements for the degree of

Master of Science in the Department of Nuclear Engineering and Health Physics

Idaho State University

Spring 2018

To the Graduate Faculty:

The members of the committee appointed to examine the thesis of MASON M. JAUSSE find it satisfactory and recommend that it be accepted.

Dr. Richard R. Brey,
Major Advisor

Dr. Kevin Konzen,
Committee Member

Dr. Rene Rodriguez,
Graduate Faculty Representative

ACKNOWLEDGEMENTS

I would like to express my gratitude and acknowledge the following individuals for their support throughout this research. I would like to thank my major advisor Dr. Richard Brey for his continued support and encouragement throughout this research and my academic career at Idaho State University. He has taught me some invaluable lessons that have well prepared me for the challenges that lie ahead in my professional career. I would like to express my upmost gratitude to Dr. Kevin Konzen for encouraging me to pursue this research and for providing me with his support and valuable advice. I greatly appreciate his willingness to share the functions that were used to assess this model. I would like to thank Dr. Rene Rodriguez for accepting the role as my graduate faculty representative and supporting me in this research.

I would like to thank my loving wife for her endless patience and support, I could not have done this without her. I also want to thank my parents for their love and support and always encouraging me to do my best.

Lastly, I would like to thank Dr. Bastian Breustedt for graciously providing me with the meticulously compiled data set of USTUR Case 0846.

TABLE OF CONTENTS

List of Figures	vii
List of Tables	ix
List of Abbreviations	x
ABSTRACT	xii
1. Introduction	1
1.1. DTPA Influence	1
1.2. Pu-DTPA Biokinetic Model	2
1.3. Research Objectives	2
1.4. Hypotheses Testing	3
2. Literature Review	5
2.1. Americium	5
2.2. Americium Biochemistry	6
2.3. Metabolic Modeling of Americium	8
2.3.1. ICRP 30: Gastrointestinal Tract Model.....	8
2.3.2. ICRP 100: Human Alimentary Tract Model	10
2.3.3. ICRP 66: Human Respiratory Tract Model	11
2.3.4. ICRP 67: Americium Systemic Model	16
2.4. DTPA	19
2.5. IDEAS Case 32	21
2.6. USTUR Case 0846	22
3. Methodology.....	24
3.1. Compartment Model Calculations	24
3.2. Am-DTPA Model.....	27
3.3. Model Optimization	28
3.3.1. Sensitivity Analysis	29
3.3.2. Uncertainty in Bioassay Measurements	30
3.4. Prediction of Intake.....	31
3.5. Statistical Analysis.....	32
3.5.1. Chi-Squared Statistic.....	32

3.5.2.	Autocorrelation Test Statistic	33
4.	Results.....	35
4.1.	IDEAS Case 32 Data	35
4.2.	Estimation of Case 32 Intake.....	36
4.3.	Model Optimization with IDEAS Case 32	40
4.3.1.	Sensitivity Analysis	42
4.3.2.	Optimized Parameters	44
4.4.	USTUR Case 0846	48
4.4.1.	Model Assessment	49
4.4.2.	Case 0846 Summary.....	52
4.5.	Hypothesis Testing	52
5.	Summary and Conclusion	54
5.1.	Summary	54
5.2.	Future Work.....	55
6.	References	56
	Appendix 1: R Functions	61

List of Figures

Fig. 2.1. ICRP 30 mathematical model used to describe the kinetics of radionuclides in the gastrointestinal tract (ICRP 1979).....	9
Fig. 2.2. Structure of the human alimentary tract model (HATM). The dashed boxes are included to show connections between the HATM and the human respiratory tract model or systemic biokinetic models (ICRP 2006).	10
Fig. 2.3. ICRP 66 compartments and clearance pathways (ICRP 1994a).....	12
Fig. 2.4. Routes of clearance from the respiratory tract (ICRP 1994b).....	13
Fig. 2.5. Compartmental model for time-dependent absorption into blood (ICRP 1994a).	14
Fig. 2.6. ICRP 67 compartmental model for plutonium, americium, and neptunium (NCRP 2008, ICRP 1993).....	18
Fig. 2.7. Structure of DTPA (Stricklin 2014).....	20
Fig. 3.1. Compartmental model example from Birchall and James (1989) and accompanying kinetic equations.....	24
Fig. 3.2. The ICRP 67 systemic model for americium coupled with the Am-DTPA biokinetic model.	27
Fig. 4.1. Compartmental model fit of ²⁴¹ Am absorption types M and S to Case 32 In-vivo lung measurements.	37
Fig. 4.2. Fecal bioassay measurements compared to the compartmental model results scaled by the MLE intake for absorption types S and M.	38
Fig. 4.3 Case 32 urine data compared to compartmental model results scaled by the MLE intake for absorption types M and S of Am-241.	39
Fig. 4.4. Modeled urine activity using Pu-DTPA transfer rates with reference model activity (dashed line) shown for comparison.	41
Fig. 4.5. Sensitivity coefficients for those complex transfer rates that have a significant influence on urinary excretion over a period of 300 days.....	43

List of Figures (continued)

Fig. 4.6. Sensitivity coefficients for those complex transfer rates that have a significant influence on early urinary excretion in Case 32 following treatment days 1, 4, and 6..... 43

Fig. 4.7. Case 32 urine excretion compared to optimized model rates (solid line) with the dashed line representing the expected excretion for a 12.2 kBq intake without DTPA enhancement. The plus signs along the x-axis indicate a chelation day..... 46

Fig. 4.8. Case 32 skeletal activity measurements compared to the Am-DTPA prediction of skeletal activity on measurement days. 47

Fig. 4.9. Case 0846 urine excretion compared to reference model (No-DTPA) and the Am-DTPA model using Am-241 absorption types M and S..... 50

Fig. 4.10. Case 0846 urine excretion from day 100 to 460 compared to reference model (No-DTPA) and the Am-DTPA model using Am-241 absorption types M and S..... 50

Fig. 4.11. Case 0846 urine excretion from day 380 to 840 compared to reference model (No-DTPA) and the Am-DTPA model using Am-241 absorption types M and S..... 51

List of Tables

Table 1. Compartmental deposition fractions for 5- μm -AMAD aerosol inhaled by reference worker (ICRP 1994a).	13
Table 2. Default absorption, transformation, and dissolution parameters (d^{-1}) (ICRP 1994a). ...	15
Table 3. Clearance rates and mean residence times for inhaled americium (type M).	16
Table 4. Transfer rates (d^{-1}) for the americium systemic model (ICRP 1993).	19
Table 5. In-vivo measurement results for IDEAS case 32.	35
Table 6. IDEAS case 32 urine and fecal bioassay data.	36
Table 7. IDEAS Case 32 modeled results summary.....	40
Table 8. Suggested complex transfer rates used in the Pu-DTPA compartment model (Konzen 2015).	40
Table 9. Sensitivity coefficients for Am-DTPA parameters for urinary excretion of americium..	42
Table 10. Recommended transfer rates for the Am-DTPA compartmental model.	44
Table 11. Comparison of model statistics using Am-241 absorption type M for 5- μm AMAD particles for Case 32 urine excretion.	46
Table 12. Case 32 skeleton activity measurements with predicted skeleton activity on measurement days.	48
Table 13. Ca-DTPA chelation treatment schedule divided into 9 contiguous periods starting in September 1967 (Rosen et al., 1980).	48
Table 14. Intake scenario 1 Case 0846 urine model statistics.....	51
Table 15. Intake scenario 2 for Case 0846 urine model statistics.	51

List of Abbreviations

AI	alveolar interstitial
Am	americium
Am-DTPA	americium complexed by diethylenetriaminepentaacetic acid in salt complex
bb	bronchioles
BB	bronchi
Bq	Becquerel
Ca	calcium
Ca-DTPA	calcium diethylenetriaminepentaacetic acid in a salt complex
CONRAD	Coordinated Network for Radiation Dosimetry
CortMarrow	cortical marrow
CortSurf	cortical surface
CortVol	cortical volume
CV95	critical value at the 95% confidence level
df	degrees of freedom
DHHS	U.S. Department of Health and Human Services
DOE	U.S. Department of Energy
DTPA	diethylenetriaminepentaacetic acid
ET	extrathoracic
FDA	U.S. Food and Drug Administration
GI	gastrointestinal
IAEA	International Atomic Energy Agency
ICRP	International Commission on Radiological Protection
IRF	intake retention fraction
kBq	kilobecquerel
λ	decay constant
LLI	lower large intestine
Ln	natural log
MLE	Maximum likelihood estimate
MBq	megabecquerel
min	minute
NCRP	National Council on Radiation Protection and Measurements
ρ	autocorrelation statistic
Pu	plutonium
Pu-DTPA	plutonium complexed by diethylenetriaminepentaacetic acid in salt complex
RE	reticuloendothelial
SI	small intestine
SF	scattering factor
ST	stomach
ST0	rapid turnover soft tissues (e.g., extracellular fluids)
ST1	intermediate soft tissues

List of Abbreviations (continued)

ST2	tenaciously retained soft tissues
Tf	transferrin
TrabMarrow	trabecular marrow
TrabSurf	trabecular surface
TrabVol	trabecular volume
μCi	microcurie
ULI	upper large intestine
μm	micron
U.S.	United States
USTUR	United States Transuranium and Uranium Registries
W_R	radiation weighting factor
W_T	tissue weighting factor
χ^2	chi-squared statistic
Zn-DTPA	zinc diethylenetriaminepentaacetic acid in salt complex

ABSTRACT

This research investigated the performance of the published Pu-DTPA biokinetic model (Konzen and Brey 2015) applied to cases involving an americium uptake influenced by DTPA treatment. Transfer rates for the Am-DTPA complex were developed from the IDEAS Case 32 urine bioassay data in an attempt to model americium metabolism under the influence of DTPA treatment. The fit of the urine data was assessed using the logarithmic chi-squared value and autocorrelation statistic, with the intake estimated using the maximum likelihood method. The Am-DTPA model provided a better fit of the Case 32 urine data than published models. The Am-DTPA model was next applied to the USTUR Case 0856 urine data and resulted in a poor fit. While not a statistically significant result, the Am-DTPA model resulted in an improved bioassay prediction, compared to reference models and suggested Pu-DTPA rates, when assessing chelation influenced urine bioassay data.

DEVELOPMENT AND APPLICATION OF AN AMERICIUM-DTPA BIOKINETIC MODEL

Thesis Abstract--Idaho State University (2018)

Key Words: americium, chelation, biokinetic

1. Introduction

Biokinetic models mathematically describe the distribution, retention, and clearance of internally deposited radioactive materials. These models are relied upon for determining the initial intake of radioactive material and the assignment of internal dose to an individual. When transuranic radionuclides are the suspected internal contaminants, medical intervention in the form of decorporation therapy is often performed. Decorporation therapy can reduce the residence time of material in the body through the enhancement of the body's excretion rate. However, these increased urinary and fecal excretion rates of the contaminant are greater than those proposed by the International Commission on Radiological Protection's (ICRP) recommended biokinetic models, thus rendering current models inaccurate under these circumstances (Konzen 2014, Davesne et al. 2016). Therefore, a need exists to continue to update these models to account for the effects of decorporation therapy.

1.1. DTPA Influence

The basic objectives of decorporation therapy are two-fold: to prevent the deposition of certain types of radioactive materials into systemic tissues, and to increase the rate of excretion of those materials from the body (Taylor et al. 2000). Currently, the most common and effective chelation agent for transuranic radionuclides is Calcium-Diethylenetriaminepentaacetic Acid (Ca-DTPA). Ca-DTPA is an organic ligand that forms water-soluble, chemically stable, ring-shaped, complexes (chelates) with metals such as plutonium and americium to form a metal-DTPA complex (Menetrier et al. 2005). An actinide-DTPA complex is generally much more stable than those formed with essential metals. Since they are excreted readily in the urine, the

spontaneous elimination of metals such as plutonium and americium is preferentially enhanced (Menetrier et al. 2005). The basic idea is to form stable and rapidly excreted complexes of the metal, which are then “masked” for the biokinetic processes of the metal itself (Breustedt et al. 2010). The complex composed of radioactive materials with DTPA enhances urinary excretion of the contaminant, preventing accumulation in organs, resulting in a dosimetric benefit but this is difficult to quantify from bioassay data using existing models.

1.2. Pu-DTPA Biokinetic Model

The Pu-DTPA biokinetic model was developed to estimate the initial intake quantity from inspection of bioassay samples influenced by chelation and to supplement standard ICRP recommended models (Konzen 2014). The Pu-DTPA biokinetic model originated from the Coordinated Network for Radiation Dosimetry (CONRAD) project and was revised to include four transitional state compartments that describe the retention of the Pu-DTPA complex using first order kinetics (Konzen and Brey 2015). These compartments were identified for the model by studying the retention of the primary tissues and organs affected by chelation (Konzen and Brey 2015). The recycling model is solved using the matrix algebra method proposed by Birchall and James (1989).

1.3. Research Objectives

The purpose of this research is to investigate the performance of the Pu-DTPA biokinetic model when applied to an uptake of americium followed by DTPA treatment. The Pu-DTPA model will be modified to account for the biochemical and physiological processes of americium metabolism and under the influence of DTPA treatment. The model transfer rates

will be developed using IDEAS Case 32 urine bioassay data and a validation performed with the urine bioassay data from USTUR Case 0846.

1.4. Hypotheses Testing

The following hypotheses will be tested in this research:

H_{1,0}: The published Pu-DTPA transfer rates cannot be optimized for americium to adequately fit the Case 32 urine bioassay data

H_{1,A}: The published Pu-DTPA transfer rates can be optimized for americium to adequately fit the Case 32 urine bioassay data.

The fit of the model to the data will be assessed using the chi-square and autocorrelation test statistics with a confidence level of $\alpha = 0.05$. A model that has a good fit will have a p-value greater than the confidence level. A p-value less than the confidence level indicates a poor fit and acceptance of the null hypothesis.

H_{2,0}: The Am-DTPA transfer rates cannot be used to predict the published mean intake in IDEAS Case 32.

H_{2,A}: The Am-DTPA transfer rates can be used to predict the published mean intake in IDEAS Case 32

The null hypotheses will be accepted if the deviation between the predicted intake activity and the published mean value is greater than 10%. In the event, the deviation between these values is less than 10%, the null hypothesis will be rejected in favor of the alternate hypothesis.

H_{3,0}: The Am-DTPA model using optimized Am-DTPA transfer rates cannot adequately fit the USTUR Case 0846 urine bioassay data

H_{3,A}: The Am-DTPA model using optimized Am-DTPA transfer rates can represent a good fit of the USTUR Case 0846 urine bioassay data

The fit of the model to the data will be assessed using the chi-square and autocorrelation test statistics with a confidence level of $\alpha = 0.05$. A model that has a good fit will have a p-value greater than the confidence level. A p-value less than the confidence level indicates a poor fit and acceptance of the null hypothesis.

2. Literature Review

2.1. Americium

Americium is a man-made transuranic element of the actinide series. It appears that Americium-241 (^{241}Am) is the only isotope of americium used in commercial applications. ^{241}Am is most commonly known as a component of ionization smoke detectors but when mixed with elemental Beryllium in order to take advantage of the (α, n) reaction, it is also used in well-logging and density gauging applications. Americium is produced in power reactor operations as well as during the detonation of nuclear weapons through neutron absorption of uranium-238 (^{238}U) or plutonium-239 (^{239}Pu) (DOE 1996, DHHS 2004). Americium-241 has a radiological half-life of 432.2 years and decays primarily through α -emission with a notable γ -emission (59.5 keV, $Y=36\%$) to ^{237}Np and a small probability (4.1E-10%) of spontaneous fission (DOE 1996).

Americium-241 is a common radionuclide found in transuranic (TRU) waste streams generated by DOE facilities (DOE 1996). Given that the specific activity of ^{241}Am is approximately 55 times higher than that of ^{239}Pu , it is clear that ^{241}Am is a potent radio-toxin. Unlike organic poisons, which the body is frequently able to metabolize, these toxic metals are either excreted or immobilized (Gorden et al. 2003). The potential for accidents during investigations of the nature of americium, or when working with fuel waste materials themselves, makes americium decorporation a valid concern (Gorden et al. 2003).

2.2. Americium Biochemistry

The stable oxidation states of americium are +3 and +4, with the most common and only state of importance in biological systems being the trivalent oxidation state (DOE 1996, Gorden et al. 2003). Upon entry into the blood stream, Am(III) has a tendency to hydrolyze, forming insoluble hydroxides or other hydroxyl species, as well as forming weak complexes with serum proteins and other ligands (ICRP 1986, DOE 1996). Durbin (2006) indicates actinide clearance from mammalian plasma is determined by its ability to form a stable complex with plasma transferrin (Tf). Those that form the most stable Tf-complexes are cleared slowly, whereas those that form only weak Tf-complexes are cleared at much faster rates (Durbin 2006). The stability of the complex is determined by the ionic radius of the actinide in relation to the size of the two binding sites on transferrin. It is anticipated that Am³⁺ ions will only bind to one of the two sites, creating a weaker complex. Whereas, Pu⁴⁺ is expected to form a more stable complex with transferrin as its ionic radius is similar to that of Fe³⁺. The weaker complex(es) are formed more slowly leading to a larger fraction leaving the plasma by diffusion to interstitial water (soft tissues) or an immediate uptake by bone and/or liver or urinary excretion (Durbin 2006).

Durbin (2006) compiled data sets of intravenously injected Am in five mammals (mouse, rat, beagle, monkey, baboon), all of which indicate a fast plasma clearance and tissue uptake of Am³⁺ with only small amounts excreted in urine in the first 24 hours. The impeded filtration through the kidneys into urine indicates that uptake of the trivalent actinides in the target tissues is rapid and/or that the major fraction of circulating actinide is bound to nonfilterable protein (Durbin 2006). Successive experiments suggest only ~30% of systemic americium forms a relatively weak bond to the blood protein transferrin ($\log K_1 = 6.3 \pm 0.7$) with the remainder

being bound to albumin, α - and γ -globulins, or to low-molecular mass species (Gorden et al. 2003, Taylor 1998, ICRP 1986).

Following entry into the blood stream, americium deposits in two principal organs, liver and bone (Taylor 1989). The initial partitioning of an actinide between deposition in bone and liver is likely to depend primarily on the relative affinities of the various circulating ligands on to the anatomical surfaces of bone or on liver cell membranes, in these situations the actinide complexes appear to be in competition with other ligands in the blood (Durbin 2006).

In bone, the binding and retention of americium is associated with the bone glycoproteins, chondroitin sulphate-protein complexes, and bone sialoproteins (Gorden et al. 2003, Chipperfield and Taylor 1970, Ansoborlo et al. 2006). The binding of americium in the skeleton, deposited on either the bone surface or incorporated into mineral bone by the osteoblasts, tends to be enhanced at resorption sites leading to the formation of areas with higher concentrations of americium (Durbin 2006, Menetrier et al. 2008). Americium is predominantly deposited on bone surfaces where some of the activity is gradually removed from the bone surface through bone restructuring processes. During such a recycling process a substantial portion of this may be returned to the blood, perhaps after temporary residence in macrophages in bone cavities, nevertheless, a portion is buried in bone volume resulting in long term retention (Leggett 1992).

When taken into the liver, americium may be taken up and/or retained in Kupffer cells and hepatocytes (Gremy et al. 2016). Kupffer cells are fixed phagocytes that destroy worn-out blood cells, bacteria and other foreign matter in the venous blood draining from the gastrointestinal

tract (Tortora and Derrickson 2009). Hepatocytes are the major functional cells of the liver, composing about 80% of the liver volume they perform a wide array of metabolic, secretory, and endocrine functions (Tortora and Derrickson 2009). A number of researchers have indicated that americium binds to the ferritin protein, enters the hepatic cells (Kupffer cells and hepatocytes), and is distributed among various organelles, with preferential accumulation in liver lysosomes (Paquet et al. 1998, Gremy et al. 2016, Taylor 1989, Menetrier et al. 2008, Lindenbaum and Rosenthal 1972). The activity is then retained in the intracellular organelles until it is excreted through either bile secretion to feces or recycled back into the blood and excreted in urine.

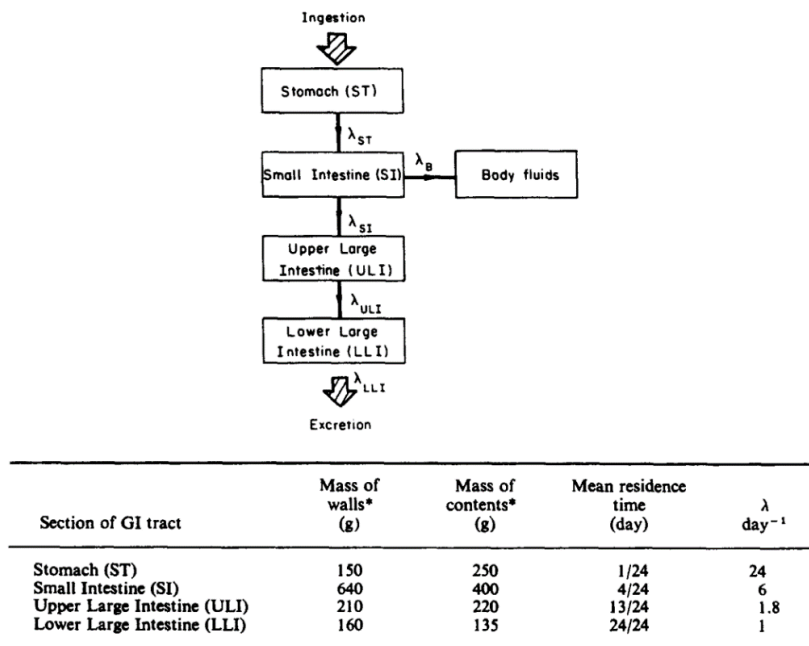
2.3. Metabolic Modeling of Americium

The following sections will briefly describe the systemic compartmental metabolic modeling of americium as recommended by the International Commission on Radiological Protection (ICRP).

2.3.1. ICRP 30: Gastrointestinal Tract Model

The ICRP 30 gastrointestinal model for the ingestion of americium, in the absence of human data, relied heavily on animal data. The absorption of all americium compounds from the gastrointestinal tract to the blood had been primarily studied in the rat. Based on the rat model, it was assumed that ingested americium compounds behaved the same as plutonium compounds and were assigned an absorption fraction (f_1) of 10^{-3} (ICRP 1979, ICRP 1988). This value was later changed in ICRP 67 to 5×10^{-4} as more human and animal data became available.

The systemic distribution and retention behavior of americium was also assumed to be like plutonium such that of the americium entering the blood, a fraction, 0.45, would be translocated to the liver and another fraction, 0.45 would be translocated to the skeleton (ICRP 1988). The fraction of americium translocated to the gonads was assumed to be 3.5×10^{-4} for the testes and 1.1×10^{-4} for the ovaries, with the remainder assumed to be excreted (ICRP 1988). It is assumed that americium deposited in the gonadal tissue is permanently retained, whereas americium deposited in the liver and skeleton has a half-time of 20 years and 50 years, respectively (ICRP 1988). Upon deposition in the skeleton, americium mainly deposits upon periosteal and endosteal bone surfaces and is then slowly redistributed throughout the volume of mineral bone (ICRP 1988). However, for the purposes of dosimetry, americium is assumed to be uniformly distributed over bone surfaces at all-time following their deposition in the skeleton (ICRP 1988). The ICRP 30 compartmental model is shown in Fig. 2.1.



* From ICRP Publication 23 (1975).

Fig. 2.1. ICRP 30 mathematical model used to describe the kinetics of radionuclides in the gastrointestinal tract (ICRP 1979).

2.3.2. ICRP 100: Human Alimentary Tract Model

ICRP publication 100 provides a human alimentary tract model (HATM) as an adjustment to the ICRP 30 GI tract model as well as complement the human respiratory tract model (HRTM) presented in ICRP publication 66 (ICRP 2006). The HATM includes compartments for the following regions: oral cavity, oesophagus, stomach, small intestine, right colon, left colon, and rectosigmoid (sigmoid colon and rectum). The model structure, shown in Fig. 2.2 allows for absorption into the blood through the oral mucosa, stomach walls, and intestines; whereas the ICRP 30 model assumes absorption to the blood occurs exclusively in the small intestine (ICRP 2006, ICRP 2015).

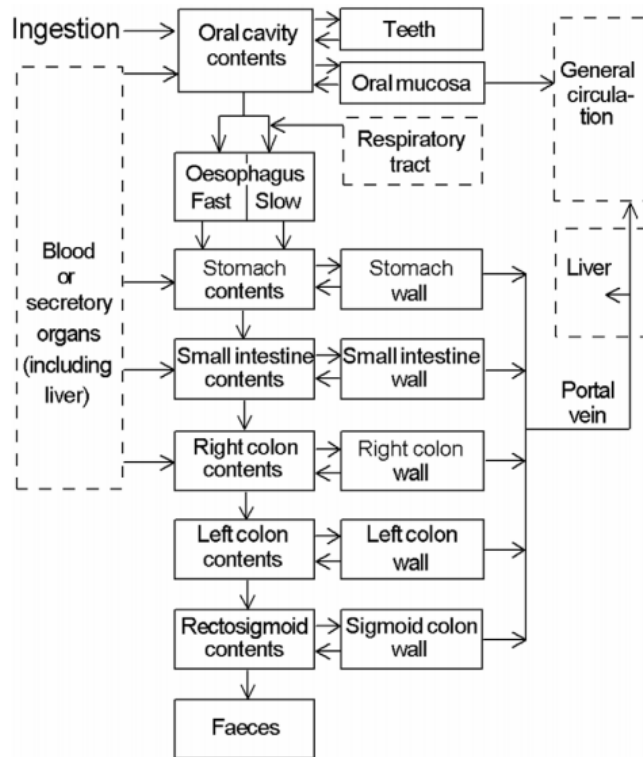


Fig. 2.2. Structure of the human alimentary tract model (HATM). The dashed boxes are included to show connections between the HATM and the human respiratory tract model or systemic biokinetic models (ICRP 2006).

The HATM provides age and gender-specific transit times for all segments of the tract depicted in the model and, for the upper segments of the alimentary tract including the oral cavity, oesophagus, and stomach. It also provides material specific transit times through these sections of the alimentary tract. (ICRP 2006). The HATM could not be used in this research effort as americium specific transfer and retention rates have not yet been published.

2.3.3. ICRP 66: Human Respiratory Tract Model

The ICRP publication 66, Human Respiratory Tract Model (HRTM), is an expansion of the lung model published in ICRP 30, designed to calculate doses to specific tissues of the respiratory tract with better accounting for the radiosensitivity of these tissues. This was motivated by the availability of increased knowledge of the anatomy and physiology of the respiratory tract and of the deposition, clearance, and biological effects of inhaled radioactive particles (ICRP 1994a). The compartmental model (shown in Fig. 2.3) represents the respiratory tract as two regions: the thoracic airways and the extrathoracic airways. The ICRP supporting guidance 3 (ICRP 2002) summarizes the HRTM compartments as follows:

- The extrathoracic (ET) airways are subdivided into ET₁, the anterior nasal passage, and ET₂, which consists of the posterior nasal and oral passages, the pharynx and larynx, together with associated lymphatic tissue (LNET).
- The thoracic regions are bronchial (BB: trachea, generation 0, and bronchi, airway generations 1–8), bronchiolar (bb: airway generations 9–15), and alveolar-interstitial (AI: the gas exchange region, airway generations 16 and beyond), together with associated lymphatic tissue (LNTH).

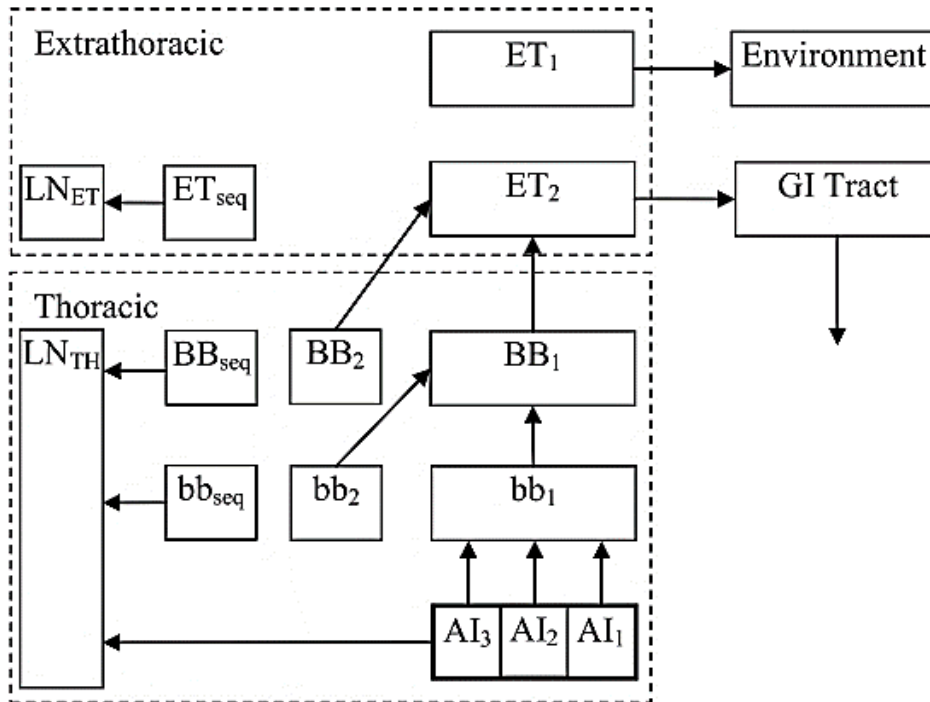


Fig. 2.3. ICRP 66 compartments and clearance pathways (ICRP 1994a).

Deposition refers to the initial processes that determine how much of the material in the inspired air remains behind after exhalation (ICRP 2002). The deposition portion of the model evaluates fractional deposition of an aerosol in each region, assuming a log-normal particle size distribution, for all aerosol sizes of particular interest (0.6 nm – 100 μ m) (ICRP 1994a, 1994b). These regional deposition fractions have been tabulated in Appendix F of ICRP 66. ICRP 66 assumes that occupational exposure, 5- μ m Activity Median Aerodynamic Diameter (AMAD) particles are representative of workplace aerosols (ICRP 1994a, 1994b). The deposition fraction in each of the lung model compartments for the occupational worker is presented in Table 1.

Table 1. Compartmental deposition fractions for 5- μ m-AMAD aerosol inhaled by reference worker (ICRP 1994a).

Region	Compartment	Compartment Fraction	5- μ m Regional Deposition	Total Assigned
ET ₁	ET ₁	1.0000	0.34	0.34
ET ₂	ET ₂	0.9995	0.4	0.3998
ET ₂	ET _{seq}	0.0005	0.4	0.0002
BB	BB ₁	0.663	0.0179	0.0118677
	BB ₂	0.33	0.0179	0.005907
	BB _{seq}	0.007	0.0179	0.0001253
bb	bb ₁	0.593	0.011	0.006523
	bb ₂	0.4	0.011	0.0044
	bb _{seq}	0.007	0.011	0.000077
Al	Al ₁	0.3	0.053	0.0159
	Al ₂	0.6	0.053	0.0318
	Al ₃	0.1	0.053	0.0053

The fraction of inhaled material deposited in the extrathoracic region (ET₁) is assumed to be cleared through extrinsic means (i.e., nose-blowing) where deposition in other regions are cleared by either particle transport or absorption processes; which are competing processes.

There are several routes of clearance from the respiratory tract as shown in Fig. 2.4.

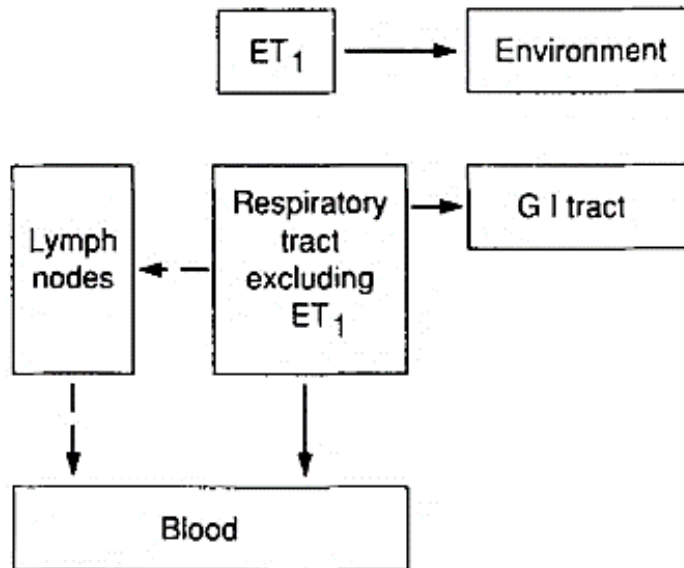


Fig. 2.4. Routes of clearance from the respiratory tract (ICRP 1994b).

Clearance of inhaled material by particle transport refers to the processes that clear material from the respiratory tract to the GI tract or to the lymph nodes and move material from one part of the respiratory tract to another (ICRP 1994). Particle transport occurs through processes such as macrophage uptake, ciliary action, and the binding to mucus. The absorption of particulates into the blood is modeled as a two-stage process: (1) the dissociation of the particles into material that can be absorbed into blood (dissolution) and (2) the uptake of material dissolved from particles or of material deposited in soluble form, a transformed state (ICRP 1994). This process is depicted in Fig. 2.5.

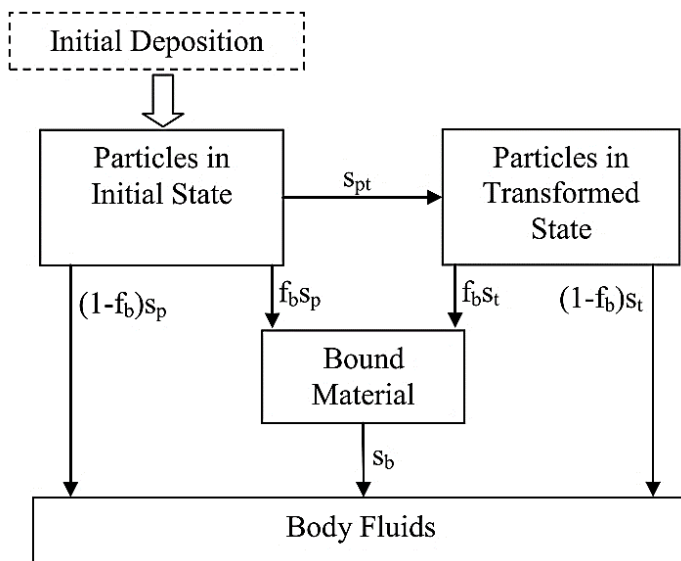


Fig. 2.5. Compartmental model for time-dependent absorption into blood (ICRP 1994a).

The ICRP (1994a) recommends that in the absence of material-specific absorption rates, the bound particle state is ignored, that is $f_b = 0$, and default parameters shown in Table 2 are to be used in the model. The absorption rates of deposited compounds are expressed as approximate half-times corresponding to one of three absorption types: fast (F), moderate (M), slow (S). All compounds of americium are considered inhalation type M (ICRP 1994b). Type M assumes that

10% is absorbed with a half-time of 10 minutes and 90% with a half-time of 140 d. There is rapid absorption of about 10% of the deposit in Bronchial (BB) and Bronchiolar regions (bb); with about 5% of the material deposited in the Extrathoracic region (ET₂), and about 70% of the deposit in the Alveolar-Interstitial (AI) region eventually reaching body fluids (ICRP 1994a, ICRP 2002).

Table 2. Default absorption, transformation, and dissolution parameters (d⁻¹) (ICRP 1994a).

Absorption Type		F (fast)	M (moderate)	S (slow)
Initial dissolution rate	S _p	100	10	0.1
Transformation rate	S _{pt}	0	90	100
Final dissolution rate	S _t	-	0.005	0.0001
Fraction to bound state	f _b	0	0	0
Uptake rate from bound state	S _b	-	-	-

The effective compartment clearance rate includes the particle translocation rate, the absorption rate into the body fluids and the rate of decay (ICRP 1994a). The effective clearance rate constant (λ_E) for each compartment is calculated using eq. (1) (ICRP 1994a).

$$\lambda_E = \lambda_{ab} + S_S + \lambda_R \quad \text{eq. (1)}$$

where,

- λ_E = effective clearance rate constant (d⁻¹)
- λ_{ab} = clearance rate constant from compartment a to compartment b (d⁻¹)
- S_S = slow absorption into the blood (0.005 d⁻¹ for Type M)
- λ_R = radiological decay constant (d⁻¹)

The effective mean residence time (MRT) can then be determined from the inverse of the compartment clearance rate (λ_E^{-1}) (ICRP 1994a). The compartmental MRT values for americium are shown in Table 3.

Table 3. Clearance rates and mean residence times for inhaled americium (type M).

Region	Compartment	To	λ_{ab} (d ⁻¹)	λ_R (d ⁻¹)	S_S (d ⁻¹)	λ_E (d ⁻¹)	MRT (d)
ET ₁	ET ₁	Environment	1	4.4E-06	5.00E-03	1.01E+00	1.00
ET ₂	ET ₂	GI Tract	100	4.4E-06	5.00E-03	1.00E+02	0.01
ET ₂	ET _{seq}	LN _{ET}	0.001	4.4E-06	5.00E-03	6.00E-03	166.54
BB	BB ₁	ET ₂	10	4.4E-06	5.00E-03	1.00E+01	0.10
BB	BB ₂	ET ₂	0.03	4.4E-06	5.00E-03	3.50E-02	28.57
BB	BB _{seq}	LN _{TH}	0.01	4.4E-06	5.00E-03	1.50E-02	66.65
bb	bb ₁	BB ₁	2	4.4E-06	5.00E-03	2.01E+00	0.50
bb	bb ₂	BB ₁	0.03	4.4E-06	5.00E-03	3.50E-02	28.57
bb	bb _{seq}	LN _{TH}	0.01	4.4E-06	5.00E-03	1.50E-02	66.65
AI	AI ₁	bb ₁	0.02	4.4E-06	5.00E-03	2.50E-02	39.99
AI	AI ₂	bb ₁	0.001	4.4E-06	5.00E-03	6.00E-03	166.54
AI	AI ₃	bb ₁	0.001	4.4E-06	5.00E-03	6.00E-03	166.54
AI	AI ₃	LN _{TH}	0.00002	4.4E-06	5.00E-03	5.02E-03	199.03
LN _{ET}	LN _{ET}	Body Fluids	-	4.4E-06	5.00E-03	5.00E-03	199.82
LN _{TH}	LN _{TH}	Body Fluids	-	4.4E-06	5.00E-03	5.00E-03	199.82

2.3.4. ICRP 67: Americium Systemic Model

ICRP 67, provides a compartmental model to describe the biokinetics of systemic plutonium, americium, and neptunium. The structure of the model was adopted from the work of Leggett (Leggett 1992). The systemic compartmental model (shown in Fig. 2.6) describes contaminant retention in the liver, skeleton, soft tissues, gonads, kidneys and bladder with the blood compartment acting as the central compartment for contaminant distribution, including urinary and fecal excretion compartments (ICRP 1993). The model divides the skeletal system into cortical and trabecular regions each of which are further sub-divided into bone surfaces, bone volume, and bone marrow compartments. Activity entering the skeletal system is initially assigned to the bone surfaces compartment then subsequently transferred to bone marrow through resorption or to bone volume by bone formation. Eventually this material is transferred from bone volume to bone marrow through bone resorption and ultimately removed from the

bone marrow compartments in a period of months (ICRP 1993). The massive soft tissue compartments represent the muscles, skin, subcutaneous fat and other soft tissues. They are modeled as three separate compartments, intermediate turnover (ST1), rapid turnover (ST0), and slow turnover (ST2), and represent the tissues ability to retain material. The soft tissue compartments ST1 and ST2 are used to represent intermediate-term retention (up to 2 years) and tenacious retention (many years) whereas the ST0 compartment is modeled as a soft tissue pool that includes extracellular fluids and exchanges material with blood over a period of hours or days (ICRP 1993). A single liver compartment (Liver 1) is used to model systemic americium. The Liver 1 compartment is viewed as a uniformly mixed pool in which a fraction, the deposited activity, is lost to the GI tract, via biliary secretion, and the remainder to the blood. The hepatic retention of americium is thought to be taken up and/or retained by the reticuloendothelial (RE) cells of the liver. The kidneys are assumed to consist of two compartments, one that transfers activity to urine and another that returns activity to blood. The blood compartment is modelled as a uniformly mixed pool that recycles activity between the soft tissues, bones surfaces, liver, kidney tissues, and gonad compartments and transfers activity to the GI tract and urinary bladder contents for excretion.

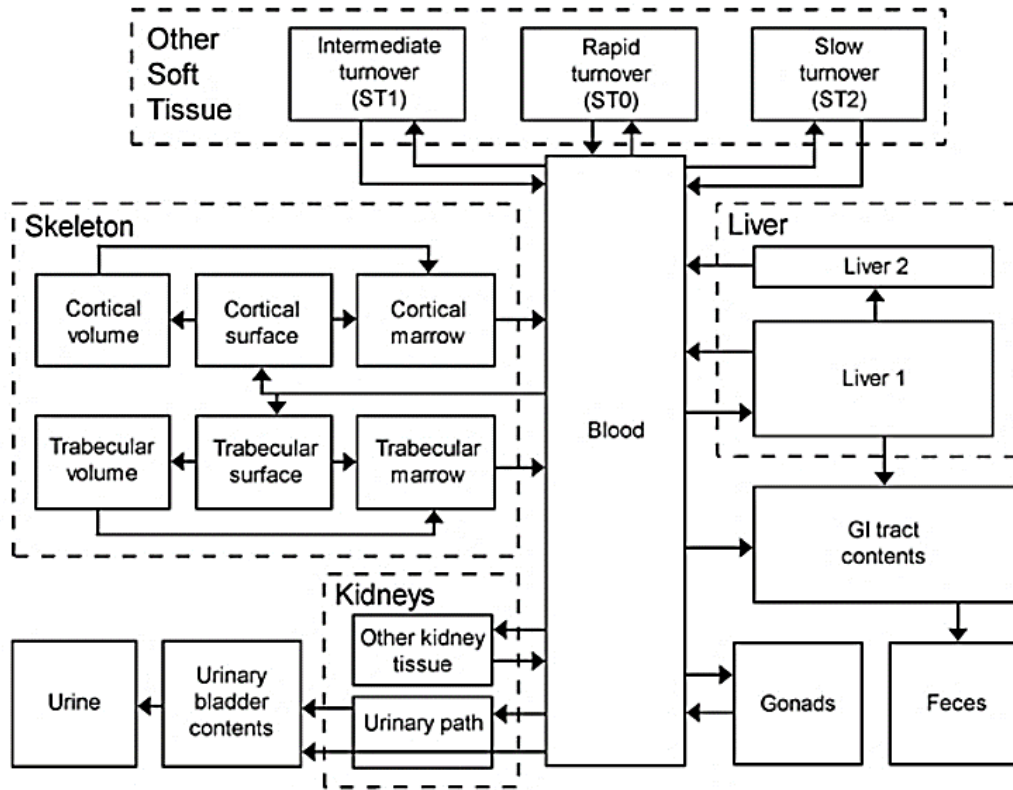


Fig. 2.6. ICRP 67 compartmental model for plutonium, americium, and neptunium (NCRP 2008, ICRP 1993).

Prior to the publication of ICRP 67, the distribution, retention and excretion of americium was assumed to be the same as that of plutonium as experimental data for americium was sparse. The biokinetics of systemic americium is now reasonably well known from animal studies and *in vivo* measurements, excretion data, and autopsy data on workers accidentally exposed to ²⁴¹Am and experimental studies on laboratory animals (NCRP 2008; Durbin 2006; ICRP 1993; Leggett 1992). The differences in the metabolic behavior of plutonium and americium are reflected in the clearance and retention parameters. For example, in the adult, it appears that the liver takes up a greater fraction of circulating americium than plutonium. The rate of loss from the liver is higher for americium than plutonium. Americium deposits more uniformly than plutonium on bone surfaces. And the rate of clearance from blood to excreta is higher for

americium than plutonium (Leggett 1992). Default compartmental transfer rates for systemic americium are provided in Table 4.

Table 4. Transfer rates (d^{-1}) for the americium systemic model (ICRP 1993).

Compartments	Adult (d^{-1})
blood to Liver 1	11.6
blood to cortical surface	3.49
blood to trabecular surface	3.49
blood to urinary bladder content	1.63
blood to kidney (urinary path)	0.446
blood to other kidney tissue	0.116
blood to ULI contents	0.303
blood to testes	0.0082
blood to ovaries	0.0026
blood to ST0	10
blood to ST1	1.67
blood to ST2	0.466
ST0 to blood	1.386
kidneys (urinary path) to bladder	0.099
other kidney tissue to blood	0.00139
ST1 to blood	0.0139
ST2 to blood	0.000019
trabecular surface to volume	0.000247
trabecular surface to marrow	0.000493
cortical surface to volume	0.0000411
cortical surface to marrow	0.0000821
trabecular volume to marrow	0.000493
cortical volume to marrow	0.0000821
cort/trab bone marrow to blood	0.0076
Liver 1 to blood	0.00185
Liver 1 to small intestine	0.000049
gonads to blood	0.00019
f1	0.0005

2.4. DTPA

Diethylene-triamine-pentaacetic acid (DTPA) is an aminopolycarboxylic acid approved by the U.S. Food and Drug Administration as a decorporation agent for transuranic radionuclides. DTPA has a very short biological half-life with 90-99% of intravenously injected DTPA being excreted, in unmetabolized form, within 24 hours in humans, canines, and rodents, as shown through use of ^{14}C -labeled DTPA (Gremy 2016, Stather 1983). Moreover, Stather (1983) found

that more than 99% of intravenously injected ^{14}C -labeled DTPA, was excreted in urine within 24 hours with less than 0.5% remaining in plasma in human volunteers. However, it was observed that about 0.1% of the administered activity was excreted on the third day and about 0.02% excreted on the seventh day. It was suggested that the small amount of DTPA was retained in the extracellular fluids and could be an explanation for elevated levels of urinary excretion of actinides in occupational persons. Initial treatment for internal radioactive contamination is usually performed through intravenous injection of pentetate calcium trisodium DTPA (Ca-DTPA) with subsequent injections of pentetate zinc trisodium DTPA (Zn-DTPA) days later. The former is normally used for initial and single administration, but since it can remove the essential bio-metals iron, manganese and zinc from the body, the zinc salt is preferred for extended or protracted administration (Stradling et al. 2005). The DTPA molecule has eight potential metal coordination sites that allow binding to a wide range of metals with high affinity (Huckle et al. 2015). DTPA has a strong binding affinity for americium under physiological conditions, as shown by its stability constant ($\text{Log } K_M$) of 22.9 (Volf 1978).

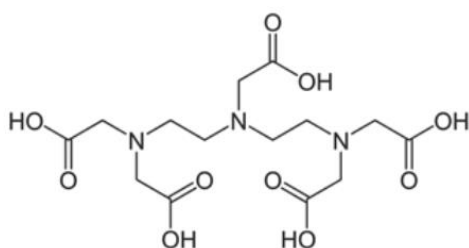


Fig. 2.7. Structure of DTPA (Stricklin 2014).

Several studies have demonstrated the effectiveness of DTPA as a chelating agent for mobilizing internalized transuranic radionuclides within humans and lab animals (Volf 1978, Durbin 2006, Taylor et al. 2000). Upon entry into the blood stream, the DTPA actively binds free

actinides yielding a stable actinide-DTPA complex. The Actinide-DTPA complex is masked from normal metabolic processes and rapidly excreted in urine. Urinary excretion can be enhanced by a factor of 100 the day following administration of DTPA and its effects can be observed for some days later (Breustedt et al. 2010).

A common modelling approach of DTPA influenced actinides has been to assume that DTPA is only distributed within the extracellular fluids and blood, without the ability to enter cells. Conversely, animal studies and human studies (e.g., Gremy et al. 2016, Roedler et al. 1989, Breistenstein et al. 1989, James et al. 2007, Fritsch et al. 2007, Carbaugh et al. 2010) indicate DTPA may also influence actinides deposited in the liver (Poudel et al. 2017). Intracellular decorporation is a possible explanation for the observed late chelation effects of deposited actinides. Research conducted by Gremy et al. (2016) suggest that DTPA can be internalized by hepatic cells where it is retained and able to decorporate previously deposited actinides or those in the process of being internalized. Modelling approaches under the assumption that DTPA can influence actinides deposited in the liver have proven to better fit the bioassay data (e.g., Konzen 2014, Konzen et al. 2016, Fritsch et al. 2007, James et al. 2007). However, the physiological mechanism for DTPA entering the cell is still controversial.

2.5. IDEAS Case 32

The IDEAS database case number 32 was used in this research. The IDEAS project evolved from a European project that was established to give guidance on internal dose assessments from monitoring data. The IDEAS guidelines, published in 2006, were developed to harmonize internal dose assessments from monitoring data. Following its publication, a working group

within the European Network - Coordinated Network for Radiation Dosimetry (CONRAD) and EURADOS was established to improve and update the IDEAS Guidelines, and to take account of recent developments in the field of internal dosimetry (Castellani et. al., 2013).

Case 32¹ involved an acute inhalation event of $^{241}\text{AmO}_2$ by a male worker. The worker was tasked with disposing of an industrial source containing 3.7 GBq (100 mCi) of ^{241}Am . The worker attempted to dismantle the source and unintentionally destroyed the capsule containing ^{241}Am in power form. The worker was immediately sent to a special radiological protection center for further evaluation and chelation therapy. The subject received 14-intravenous injections of Ca-DTPA over a period of 294 days, over-which urine and fecal bioassay data were collected. Intake estimations and dose evaluations were performed by 13 laboratories, using suggested ICRP models and derived functions to account for the DTPA treatment. The data and results were compiled and presented in IAEA (1999).

2.6. USTUR Case 0846

The United States Transuranium and Uranium Registries (USTUR), a research program dedicated to the studies of internally deposited actinides, is operated by Washington State University College of Pharmacy. The USTUR provides dosimetric data, obtained from voluntary whole-body donors whom have had an accidental intake of actinide elements, to interested research scientists.

¹ Case 32 data provided in IDEAS database available online at: <http://www.sckcen.be/ideas/>; accessed on May 5th, 2017.

USTUR Case 0846² involved an accidental inhalation of ²⁴¹Am aerosol while preparing foils, each containing up to 200 mg (\approx 500 mCi) of americium oxide. This work was conducted inside a glovebox where they were then to be compacted (Rosen et al. 1980). The individual performed these tasks for a period of 2 to 3 years until α -activity was discovered in his first *in vivo* urine analysis during May of 1967, over-which he was then removed from the work area to prevent further exposure (Rosen et al. 1980). It is presumed that the exposure first occurred in the beginning of the second year of work, when the compaction of the foils began, but this is not known for certain (Rosen et al. 1980). The individual began weekly decorporation therapy with Ca-DTPA in September of 1967 and this continued through 1974 with few interruptions (Rosen et al. 1980). The case initially estimated a total body burden of 1.8 μ Ci (66.6 kBq) of ²⁴¹Am (Rosen et. al 1980, Fasiska et al. 1971). This case has been extensively studied (Fasiska et al. 1971, Slobodien et al. 1973, Horm 1973, Rosen et al. 1980, Brodsky et al. 2004, Breustedt et al. 2016) and provides a unique insight into the later term removal of americium enhanced by decorporation therapy.

The Case 0846 data and documents used in this research effort were provided by the USTUR, which included an excel file containing excretion data compiled by Dr. Bastian Breustedt.

² USTUR Case 0846 data was requested and obtained from the U.S. Transuranium and Uranium Registries on

3. Methodology

The Pu-DTPA biokinetic model (Konzen 2014, Konzen and Brey 2015) was used as a template to develop the Am-DTPA biokinetic model. The compartments used to describe the biokinetics of complexed Pu were assumed to also be representative of the biokinetics of the Am-DTPA complex. The following sections will describe the mathematical methods used to solve the model.

3.1. Compartment Model Calculations

Birchall and James (1989) proposed linear algebraic methods to solve compartmental models involving recycling. This concept is illustrated in Fig. 3.1 using a simple compartmental model where the $x_1(t) \dots x_4(t)$ represent initial quantities of material in the respective compartments and letters represent the transfer rates among these compartments.

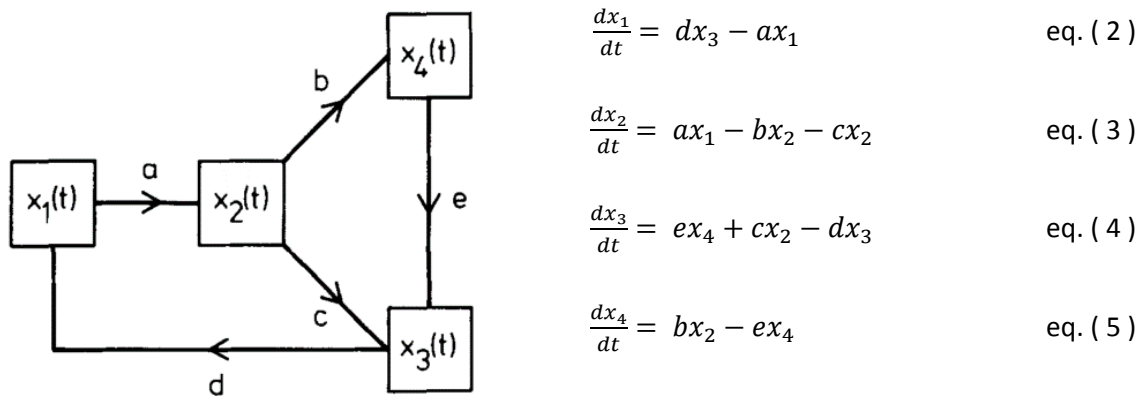


Fig. 3.1. Compartmental model example from Birchall and James (1989) and accompanying kinetic equations.

Birchall and James (1989) suggest the compartmental model can be represented by a rate matrix with the initial quantities located on the diagonal elements and the transfer rates located on the off-diagonal elements. The compartmental model represented in rate matrix form with the source compartments as rows and the destination compartments as columns is shown below.

$$\mathbf{R}_{ij} = \begin{bmatrix} x_1(0) & a & 0 & 0 \\ 0 & x_2(0) & c & b \\ d & 0 & x_3(0) & 0 \\ 0 & 0 & e & x_4(0) \end{bmatrix}$$

The rate matrix **[R]** is created to represent the biokinetic model. Each element (R_{ij}) of the matrix contains a numerical value r_{ij} , the translocation rate constant from compartment i to compartment j , and each diagonal element R_{ii} contains the initial amount $x_i(0)$ in compartment i . The kinetic equations used to describe this model are combined and represented by eq. (6).

eq. (6)

$$\frac{dx_i}{dt} = \sum_{\substack{j=1 \\ j \neq i}}^N r_{ji}x_j - x_i \sum_{\substack{j=1 \\ j \neq i}}^N r_{ij}$$

The combined kinetic equation is transformed into an **[A]** matrix as follows:

Let: $a_{ji} = r_{ji}$ (off-diagonal elements are transfer rates and remain unchanged)

eq. (7)

$$a_{ii} = - \sum_{\substack{j=1 \\ j \neq i}}^N r_{ij}$$

The initial quantities along the diagonal of the **A** matrix are transformed using eq. (7) and yield the following **A** matrix.

$$\mathbf{A} = \begin{bmatrix} -a & 0 & d & 0 \\ a & -(b+c) & 0 & 0 \\ 0 & c & -d & e \\ 0 & b & 0 & -e \end{bmatrix}$$

Substitution of r_{ji} and r_{ij} with a_{ij} and a_{ii} into eq. (6) yields,

$$\frac{dx_i}{dt} = \sum_{\substack{j=1 \\ j \neq i}}^N a_{ij}x_j + a_{ii}x_i = \sum_{j=1}^N a_{ij}x_j = [\mathbf{A}]x$$

Therefore, final quantities at any time can be solved using eq. (8):

eq. (8)

$$x(t) = e^{[\mathbf{A}]t} \cdot x(0)$$

And the total transformations is determined by integrating eq. (9) and multiplying by the radioactive decay constant.

eq. (9)

$$u(t) = \lambda_R [\mathbf{A}]^{-1} [e^{[\mathbf{A}]t} - I] x(0)$$

The R environment³ was used to create functions utilizing these matrix methods to evaluate the Am-DTPA model. Konzen (2014, 2015) developed a suite of functions to assist in the solving the model. These functions were modified to be representative of americium and are described in Appendix 1.

³ R Core Team (2017). R: A language and environment for statistical computing. R Foundation for Statistical Computing, Vienna, Austria. URL <https://www.R-project.org/>.

3.2. Am-DTPA Model

The complexation and excretion of americium by DTPA is modeled using the four transitional compartments, *ST0.d*, *ST1.d*, *Blood.d*, and *Liver.d*, proposed for the Pu-DTPA model Konzen and Brey (2015). The transitional compartments supplement the ICRP 67 (1993) systemic model as shown in Fig. 3.2.

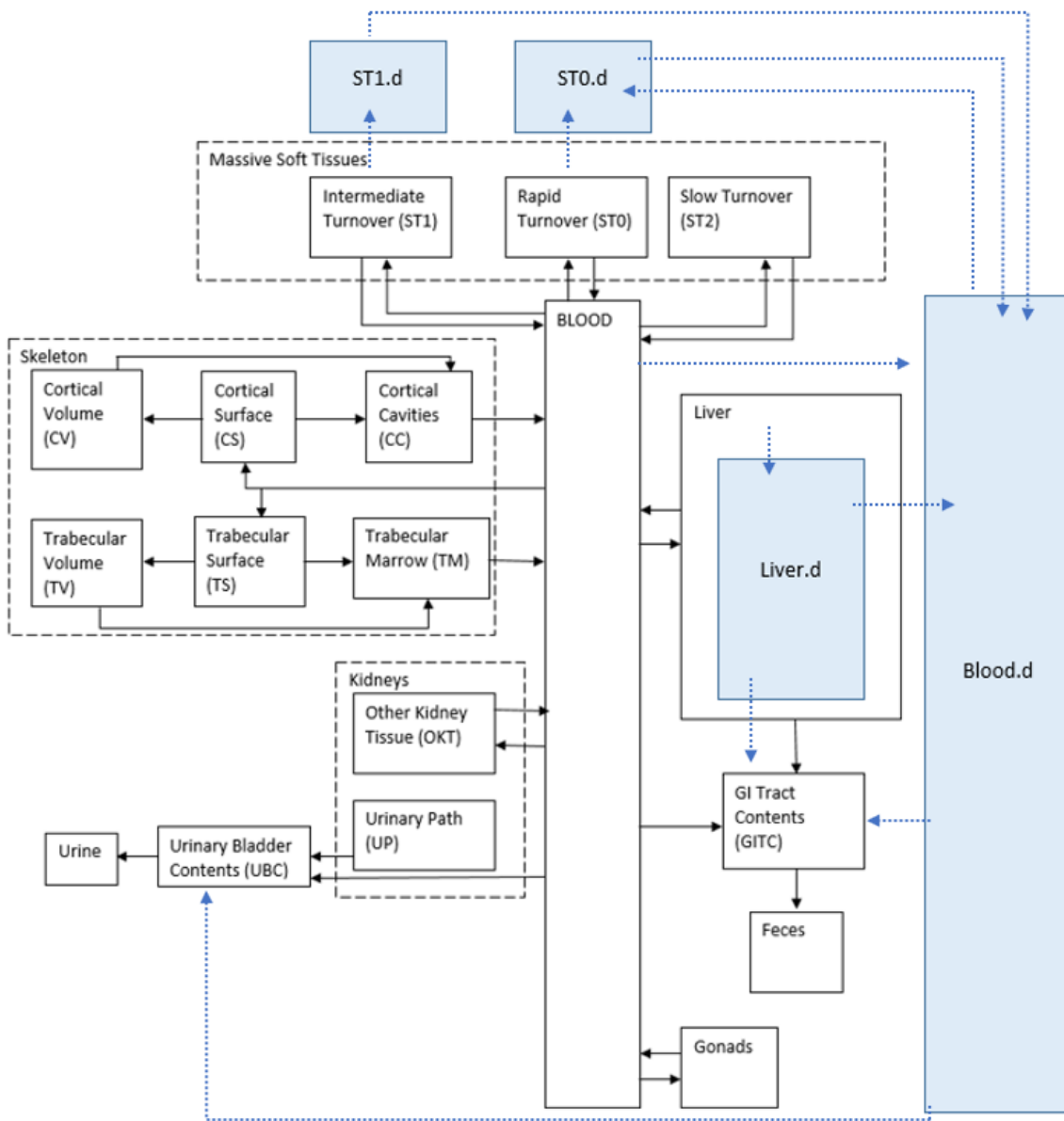


Fig. 3.2. The ICRP 67 systemic model for americium coupled with the Am-DTPA biokinetic model.

Upon administration of intravenous DTPA, it is assumed DTPA enters the blood compartment where it competes with metabolic processes and blood proteins to form a Am-DTPA complex. The complex is then modeled using the transitional compartments. The *Blood.d* compartment exchanges DTPA and Am-DTPA with the rapid turnover soft tissues (*ST0.d*) compartment to represent the physiological rapid circulation between the blood and the soft tissues and excrete the complex via the urinary bladder or the GI tract. This is intended to account for the increased urinary excretion of americium within the first 24 hours following treatment. The literature indicates that chelation treatment affects urinary excretion data for a period of weeks to months with a suggested 2 to 3% of the decorporation occurring after the first day (Fritsch et al. 2010, Carbaugh et al. 2010, Poudel et al. 2017, Davesne et al. 2016, LaBone 1994). Hence, the *Liver.d* and *ST1.d* compartments are intended to model the late effects of chelation allowing for DTPA to influence retained americium in the liver and intermediate turnover soft tissues.

3.3. Model Optimization

The Am-DTPA transfer rates were optimized to fit the urine data from IDEAS Case 32. The transfer rates recommended for the Pu-DTPA model, shown in Table 3.1, were used as a starting point for optimization. The urine excretion data set will be used to develop transfer rates for the Am-DTPA model and then applied to USTUR Case 0856 urine data for evaluation.

Table 3.1. Recommended transfer rates for the Pu-DTPA biokinetic model (Konzen 2015).

Compartment Pathway	Transfer Rate (d ⁻¹)	Compartment half-time	Compartment Pathway	Transfer Rate (d ⁻¹)	Compartment half-time
ST0 to ST0.d	3.65	273.5 minutes	Blood.d to ULI	4	249.5 minutes
ST1 to ST1.d	1.925	518.5 minutes	Blood.d to Bladder	45.7	21.8 minutes
Blood to Blood.d	1.378	724.3 minutes	Liver to Liver.d	2.2	453.7 minutes
ST0.d to Blood.d	300	3.3 minutes	Liver.d to Blood.d	0.067	10.3 days
ST1.d to Blood.d	0.12	5.8 days	Liver.d to SI	0.067	10.3 days
Blood.d to ST0.d	145	6.9 minutes			

3.3.1. Sensitivity Analysis

A sensitivity analysis was applied to the Am-DTPA model to identify the model parameters that have the largest influence on urinary excretion. This method was suggested by Luciani et al. (2001) to determine a biokinetic models transfer rates, and in a certain way physiological processes, which could be the cause of significant deviations between measurements and model predictions. The sensitivity coefficient (S_i) is defined as the ratio of the relative change of the excretion rate (u) to the relative change of the respective transfer parameter (λ_i) and is calculated using eq. (10).

eq. (10)

$$S_i = \frac{\delta u \lambda_i}{\delta \lambda_i u}$$

As time-dependent transfer rates are used, only numerical approximations to the partial derivative can be calculated, using a finite difference method as shown by eq. (11). Analysis conducted by Luciani et al. (2001) confirmed that the increment of 1% (0.01) is small enough to represent a valid approximation to the derivative and, at the same time, is large enough to avoid numerical rounding problems.

eq. (11)

$$S_i = \frac{\Delta u}{\Delta \lambda_i} \frac{\lambda_i}{u}; \Delta \lambda_i = 0.01 \lambda_i$$

The *sens* function, developed by Konzen (2014), was used to evaluate the transfer rates which had the most influence on urinary excretion at a provided time *t*. The *sens* function performs the sensitivity analysis over the rate matrix for specified compartments for a defined time period and is shown in Appendix 1. All parameters with a sensitivity coefficient (S_i) greater than the absolute value of 0.1 are considered to have a significant effect on the urinary excretion at the time of interest (Luciani et al. 2001). The absolute value of 0.1 was chosen as the level of significance such that a 1% perturbation in the transfer parameter (λ_i) resulting in a 1% change in the excretion rate would be considered to have a significant influence (Khursheed and Fell 1997).

3.3.2. Uncertainty in Bioassay Measurements

The IDEAS scattering factor (SF) is a measure of the uncertainty of an individual monitoring value. The IDEAS guidelines (Castellani et al. 2013) divides uncertainty into two categories Type A and Type B. Type A describes uncertainties in the counting statistics associated with each monitoring value and follows a Poisson distribution. Type B accounts for all other uncertainties associated with *in-vivo* measurements such as detector positioning and calibration. The IDEAS guidelines assume that the overall uncertainty of an individual monitoring value can be described in terms of a log-normal distribution and the scattering factor (SF) is defined as its geometric standard deviation. A compiled uncertainty analyses lead to the assumption that Type B uncertainties have the largest influence on the uncertainty of bioassay measurements.

The scattering factor for a normalized 24-hour urine samples was given as 1.3 to 1.8, with an average of 1.6 (Castellani et al. 2013). The SF for a 24-hour fecal sample ranged between 2 to 4, with an average of 3 (Castellani et al 2013). The IDEAS case 32 data also include lung measurements, the guidelines recommend a SF of 1.4 for in-vivo measurements of ²⁴¹Am 59.5-keV gamma-rays (Castellani et al. 2013). The SF values used in this research effort are the average values suggested by Castellani et al. 2013, 1.6, 3.0, and 1.4, respectively.

3.4. Prediction of Intake

The maximum likelihood method was used to predict the intake experienced by IDEAS Case 32 and USTUR Case 0846. The likelihood function is the probability density function of observing the measurement data given the intake and model parameter values (Castellani et al. 2013). The maximum likelihood estimate (MLE) of intake is calculated using eq. (12).

eq. (12)

$$\ln(I) = \frac{\sum_{i=1}^n \frac{\ln(I_i)}{[\ln(SF_i)]^2}}{\sum_{i=1}^n \frac{1}{[\ln(SF_i)]^2}}$$

Where,

$$I_i = \frac{M_i}{m(t_i)}$$

Since the scattering factor is held constant for each type of measurement, the maximum likelihood estimate of intake becomes,

eq. (13)

$$\ln(I) = \frac{1}{n} \sum_{i=1}^n \ln(I_i) = \ln \left[\left(\prod_{i=1}^n I_i \right)^{\frac{1}{n}} \right]$$

$$I = \sqrt[n]{\prod_{i=1}^n I_i}$$

Which is the geometric mean of the point estimate intakes (I_i) (Castellani et al. 2013).

3.5. Statistical Analysis

The Am-DTPA model fit to IDEAS Case 32 bioassay data was assessed using the chi-squared and autocorrelation test statistics as suggested in the IDEAS Guidelines.

3.5.1. Chi-Squared Statistic

It is assumed that each measurement, M_i , is taken from a lognormal distribution with a scattering factor of SF_i , and the product $Im(t_i)$ is the predicted excretion value and R_i are the normalized residuals, as shown in eq. (14).

eq. (14)

$$\chi_0^2 = \sum_{i=1}^n \left(\frac{\ln(M_i) - \ln[Im(t_i)]}{\ln(SF_i)} \right)^2 = \sum_{i=1}^n R_i^2$$

The IDEAS guidelines propose that the fit is inadequate if the p-value < 0.05 or if the fit displayed graphically looks unreasonable by eye (Castellani et al. 2013). A graphically unreasonable fit is an overestimation or underestimation of a long series of data. The χ^2 test uses assumed uncertainties (SF_i) that if overestimated results in a small χ^2 and accepted bad fit or underestimated result in a large χ^2 and a rejected good fit. This can be resolved by examining the serial correlation in the residuals using the autocorrelation coefficient statistic, as the autocorrelation statistic has the advantage of being relatively insensitive to assumed measurement uncertainties (Castellani et al. 2013, Puncher et al. 2007).

3.5.2. Autocorrelation Test Statistic

The autocorrelation test statistic (ρ) provides an objective means of detecting the bias in the residual sequence caused by fitting an inadequate model to bioassay data (Puncher et. al 2013). The ρ test is insensitive to the magnitudes of the uncertainties assumed in the bioassay data and can identify underestimation or overestimation trends, unlike the χ^2 test statistic. The autocorrelation statistic is calculated using eq. (15).

eq. (15)

$$\rho = \frac{\sum_{i=1}^{n-1} R_i R_{i+1}}{\sum_{i=1}^n R_i^2} \quad (-1 < \rho < 1)$$

Where,

$$R_i = \frac{\ln(M_i) - \ln(I m(t_i))}{\ln(SF)}$$

Where M_i is the i th measurement made at time t_i after the intake; I is the estimated intake, $m(t_i)$ is the modeled bioassay value for time t after the intake; and SF is the geometric standard deviation (scattering factor) assumed to represent the uncertainty of the data (Puncher et. al 2013). The autocorrelation test ranges from -1 to 1 and is based on the upper tail test of a normal distribution, evaluated at the critical value of the 95% confidence limit. The critical value is determined at $\mu \pm 1.96\sigma$. A ρ less than the critical value indicates an acceptable fit.

4. Results

4.1. IDEAS Case 32 Data

The IDEAS case 32 data set included in-vivo measurements of the respiratory tract, liver, and skeleton as well as urine and fecal excretion data spanning 294 days. The in-vivo measurements reported above the provided minimum detectable activity are shown in Table 5 and the urine and fecal excretion data are shown in Table 6.

Table 5. In-vivo measurement results for IDEAS case 32.

Days	Results (Bq)	Uncertainty (Bq)	Measurement	Notes
0	533	53	Resp. tract	1g Ca-DTPA administered
1	435	44	Resp. tract	
4	376	38	Resp. tract	1g Ca-DTPA administered
4	26	11	Skeleton	
21	313	31	Resp. tract	1g Ca-DTPA administered
28	312	31	Resp. tract	1g Ca-DTPA administered
53	211	21	Resp. tract	
91	130	13	Resp. tract	2g Zn-DTPA administered
91	9	4	Liver	
91	30	11	Skeleton	
207	47	5	Resp. tract	2g Zn-DTPA administered
207	36	11	Skeleton	
278	43	4	Resp. tract	
278	46	11	Skeleton	

Table 6. IDEAS case 32 urine and fecal bioassay data.

Day	Urine Bioassay (Bq)	Fecal Bioassay (Bq)	Notes	Day	Urine Excretion (Bq)	Fecal Excretion (Bq)	Notes
1	8.65	215	1g Ca-DTPA day before	77	0.548		
2	2.92	86.2		78	0.929	0.365	
3	2.66	8.01		88		0.27	
4	1.68	4.13	1g Ca-DTPA	89	0.275	0.387	
5	3.24	3.91		90	0.343	0.039	
6	1.28	0.033	1g Ca-DTPA	91	0.51	0.405	2g Zn-DTPA
7	2.49	0.199		92	2.5		
8	2.05	0.469		93	1.17	0.369	
9	2.14	1.51		94	1.4		
10	1.63	0.169		95	1.87	1.2	
11	2.3	0.295		110	1.44	0.224	2g Ca-DTPA day before
12	1.66	0.529		111	1.07	0.289	
13	1.43			112	1.38	1.18	
14	1.89	0.41		113	1.74	0.433	
15	2.75	0.531	1g Ca-DTPA	125	0.65		
16	2.65			126	0.64		
17	2.02	0.529		141	0.265		2g Zn-DTPA
18	1.87	0.353	1g Ca-DTPA	142	1.56	0.049	
19	2.57			143	0.905	0.33	
20	2.65	0.8		169	0.258		2g Ca-DTPA
21	1.43	0.83	1g Ca-DTPA	170	1.41	0.06	
22	2.7			171	0.566	0.321	
23	2.09	0.9		172	0.953	0.396	
24	2.44	0.233		207	0.084		2g Zn-DTPA
25	1.98	0.366	1g Ca-DTPA	208	0.733	0.044	
26	2.4	0.398		209	0.836	0.0858	
27	2.24			210	0.291	0.309	
28	2.01	0.566	1g Ca-DTPA	221	0.165		
29	3.26	0.219		237	0.081		
30	1.41	0.253		238	0.887		
31	2.3	0.168		239	0.288	0.042	
32	1.49	0.653		240	0.203		
51	1.23	0.415		272	0.0415		2g Zn-DTPA
52	1.43			273	0.733	0.0912	
53	1.15	0.746		274		0.131	
61		0.136		275	0.29		
62	0.562	0.103		276	0.328		
63	1.18			277	0.111	0.25	
64	0.72	0.113		294	0.0564		
76	0.418	0.138					

4.2. Estimation of Case 32 Intake

In-vivo lung measurements

The in-vivo lung measurements were selected to estimate the initial intake since they were not expected to be affected by chelation. The measurement data were analyzed using ^{241}Am

reference values for absorption types M and S for 5- μm AMAD particles in the coupled ICRP 30, 66, and 67 models. These data are shown in Fig. 4.1.

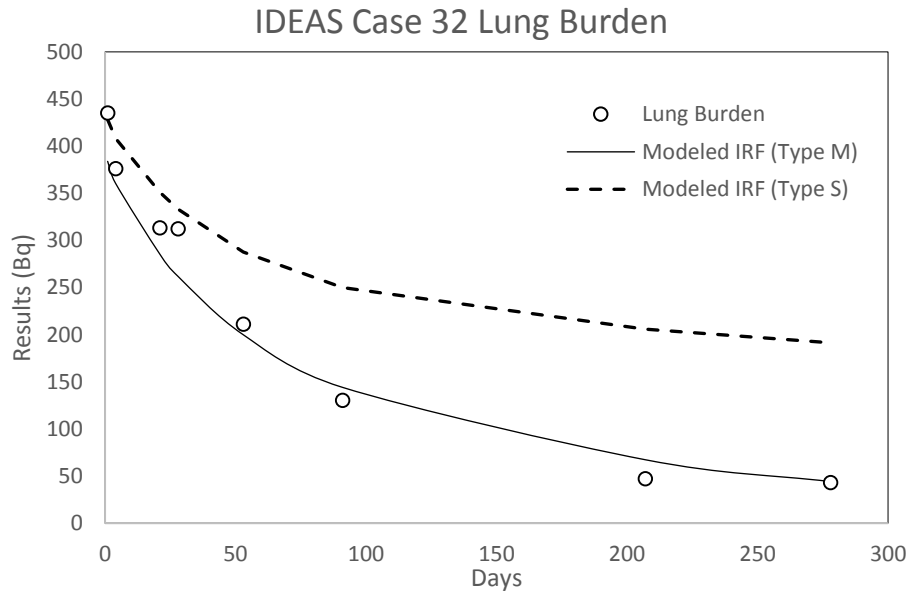


Fig. 4.1. Compartmental model fit of ^{241}Am absorption types M and S to Case 32 *In-vivo* lung measurements.

Absorption type M resulted in the best fit of the *in-vivo* lung measurements. The maximum likelihood estimate (MLE) of intake was calculated as 6,682 Bq with an IDEAS chi-squared value (χ^2) of 1.77 and autocorrelation statistic (ρ) of 0.38. The model of absorption type S predicted a MLE intake of 3961 Bq ($\chi^2 = 24.51$, $\rho = 0.62$). The fit of the data is considered inadequate since the ρ exceeds the critical value (CV) at the 95% confidence level for this data set, which was calculated as 0.34. However, type M is more representative of this data set than type S, the assumed absorption type M will be used in this research.

Fecal data

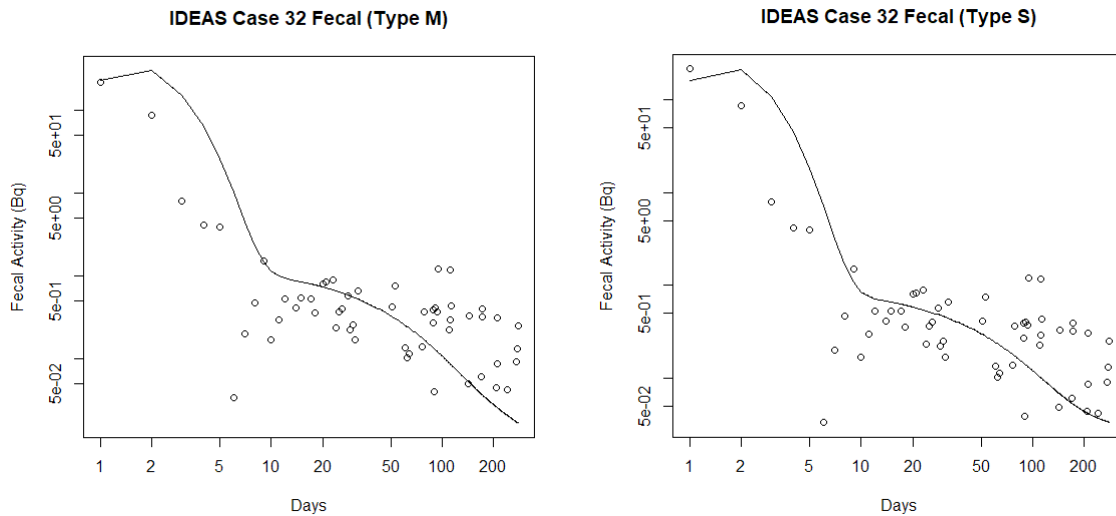


Fig. 4.2. Fecal bioassay measurements compared to the compartmental model results scaled by the MLE intake for absorption types S and M.

The case fecal data were also modeled to estimate the initial intake; even though fecal data were expected to have been influenced by DTPA. These data are shown Fig. 4.2.

The reference models predicted an intake of 1,325 Bq ($\chi^2 = 88.23$, $\rho = 0.57$, $CV = 0.195$) for absorption type S and 1,975 Bq ($\chi^2 = 116.9$, $\rho = 0.67$, $CV = 0.195$) for absorption type M. The reference models do not exhibit a good fit of the data and cannot adequately predict the published intake for Case 32.

Urine data

The urine data are strongly influenced by chelation and cannot be used to assess an intake. However, the case data were assessed using the reference models for both absorption types M and S for later comparison. The results are shown in Fig. 4.3.

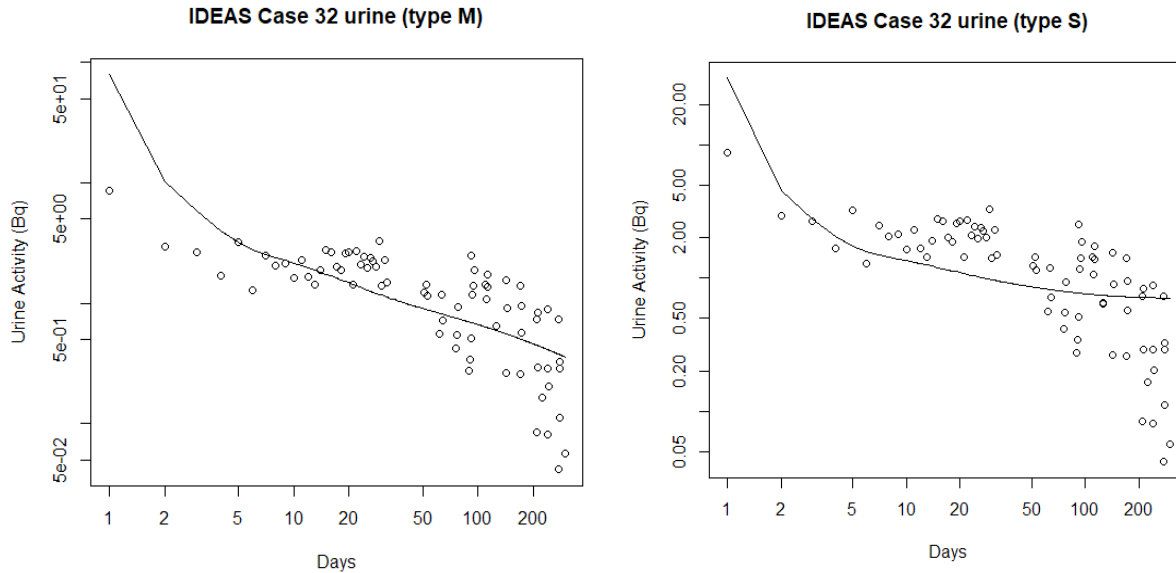


Fig. 4.3 Case 32 urine data compared to compartmental model results scaled by the MLE intake for absorption types M and S of Am-241.

The reference coupled ICRP models predicted an intake of 44,608 Bq ($\chi^2 = 203.22$, $\rho = 0.29$, $CV=0.17$) for type M and 1,775,665 Bq intake ($\chi^2 = 266.24$, $\rho = 0.45$, $CV=0.17$) for type S. The urine data, modeled as type M, will be used for further analysis and optimization of the Am-DTPA compartmental model since it has a better fit than type S.

A summary of the case intake assessment is shown in Table 7. The average intake for case 32 was published in IAEA-TECDOC-1071 as 4.14 ± 3.12 kBq. The relative standard deviation is 75% and the spread of intake estimates can be attributed to the varied AMAD values used by the 13-different laboratories that assessed this case. The average intake estimated by assessors that used a 5- μm AMAD particle was 7.22 ± 1.69 kBq. The estimated lung burden using absorption type M and 5- μm AMAD particle proved to be the best fit of the case lung measurements predicting a 6,681 Bq intake.

Table 7. IDEAS Case 32 modeled results summary.

	Type	MLE Intake (Bq)	χ^2	ρ	Critical Value
Lung Measurements	M	6681	1.8	0.38	0.34
Lung Measurements	S	3961	24.5	0.62	0.34
Fecal	M	1975	116.9	0.67	0.19
Fecal	S	1325	88.2	0.57	0.19
Urine	M	4.46E+04	203.2	0.29	0.17
Urine	S	1.78E+06	266.2	0.45	0.17

4.3. Model Optimization with IDEAS Case 32

The Case 32 urine excretion data were selected to optimize the Am-DTPA compartmental model. The Am-DTPA model was initially investigated using the suggested Pu-DTPA transfer rates (Konzen 2015), shown in Table 8. These rates were developed and optimized for the Pu-DTPA complex and are used in this research to establish an initial fit of the Case 32 urine data.

Table 8. Suggested complex transfer rates used in the Pu-DTPA compartment model (Konzen 2015).

Compartment Pathway	Transfer Rate (d ⁻¹)	Compartment half-time	Compartment Pathway	Transfer Rate (d ⁻¹)	Compartment half-time
ST0 to ST0.d	3.65	273.5 minutes	Blood.d to ULI	4	249.5 minutes
ST1 to ST1.d	1.925	518.5 minutes	Blood.d to Bladder	45.7	21.8 minutes
Blood to Blood.d	1.378	724.3 minutes	Liver to Liver.d	2.2	453.7 minutes
ST0.d to Blood.d	300	3.3 minutes	Liver.d to Blood.d	0.067	10.3 days
ST1.d to Blood.d	0.12	5.8 days	Liver.d to SI	0.067	10.3 days
Blood.d to ST0.d	145	6.9 minutes			

Treatment with Ca-DTPA took place on days 1, 4, 6, 15, 18, 21, 25, 28, 109, and 169. Treatment with Zn-DTPA took place on days 91, 141, 207, and 272. This research did not make a distinction between Ca- and Zn-DTPA for these treatment days; which were assumed to behave as Ca-DTPA kinetics. Treatment days were increased by one to represent the 24-hour enhancement on the collection day. The modeled Case 32 urine activity using the Pu-DTPA transfer rates is shown in Fig. 4.4.

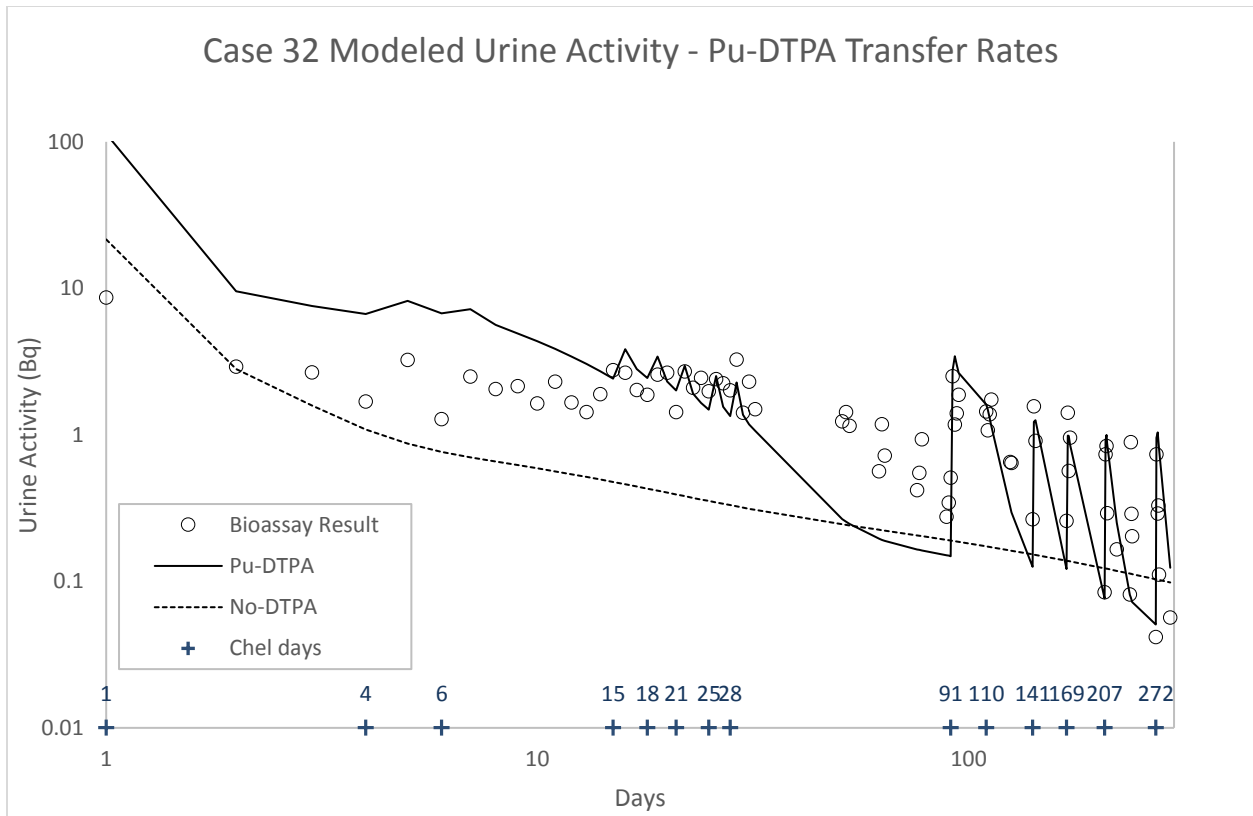


Fig. 4.4. Modeled urine activity using Pu-DTPA transfer rates with reference model activity (dashed line) shown for comparison.

The modeled Case 32 urine using ICRP reference parameters (No-DTPA), shown as the dashed line, is also provided for comparison. The maximum likelihood estimate of intake was calculated as 12,946 Bq ($\chi^2 = 299.8$, $\rho = 0.71$, $CV = 0.17$) using Pu-DTPA suggested transfer rates. The model is overestimating the urine activity for day 1 by approximately 105 Bq and by 3.16 Bq on average for days 2 through 15. The model then fractionally underestimates the urine activity on days 29–90 by an average 0.60 Bq. The autocorrelation statistic showed a temporal bias in the model, indicating a poor fit of the urine data. However, the fit of the data is better than not accounting for chelation as the spikes in excreted urine activity following chelation days can be observed.

4.3.1. Sensitivity Analysis

A sensitivity analysis was applied to the modeled urine data to identify which of the Am-DTPA compartment pathways has the largest influence on urine excretion over the collection period. These data are shown in Table 9.

Table 9. Sensitivity coefficients for Am-DTPA parameters for urinary excretion of americium.

Pathway		Accumulated Urine (Days)								
		1	5	10	50	100	150	200	250	300
Blood	Blood.d	0.09	0.30	0.04	0.03	0.03	0.03	0.03	0.03	0.03
ST1.d	Blood.d	0.01	0.02	0.04	0.00	0.00	0.00	0.00	0.00	0.00
Liver.d	GI SI	0.00	-0.16	-0.06	-0.15	-0.15	-0.15	-0.15	-0.16	-0.16
Liver.d	Blood.d	0.03	0.18	0.19	0.16	0.16	0.16	0.16	0.16	0.16
Blood.d	GI ULI	-0.07	-0.32	-0.07	-0.07	-0.07	-0.07	-0.07	-0.07	-0.07
Blood.d	Bladder	0.07	0.46	0.07	0.07	0.07	0.07	0.07	0.07	0.07
Liver	Liver.d	0.02	0.04	0.01	0.00	0.00	0.00	0.00	0.00	0.00
ST0	ST0.d	0.17	0.07	0.06	0.05	0.05	0.05	0.05	0.05	0.05
ST1	ST1.d	0.00	0.01	0.06	0.00	0.00	0.00	0.00	0.00	0.00

The ST0 to ST0.d pathway had the most positive influence on urinary excretion indicating that an increase in this pathway transfer rate would lead to a larger predicted urine excretion value for day 1. Whereas the Blood.d to the GI ULI pathway had the most negative influence for day 1 indicating an increase in the transfer rate would lead to a decreased in the predicted urine activity value. The Liver.d to Blood.d pathway has the most positive influence from days 10 through 300 with competition from the Liver.d to GI SI pathway. The sensitivity parameters of these pathways were extended to +0.05 and -0.05 and those transfer rates are displayed graphically in Fig. 4.5 and Fig. 4.6. Figure 4.6 shows the most sensitive urinary excretion pathways for the first collection days 1, 5, 7, and 10 following treatment days 0, 4, and 6.

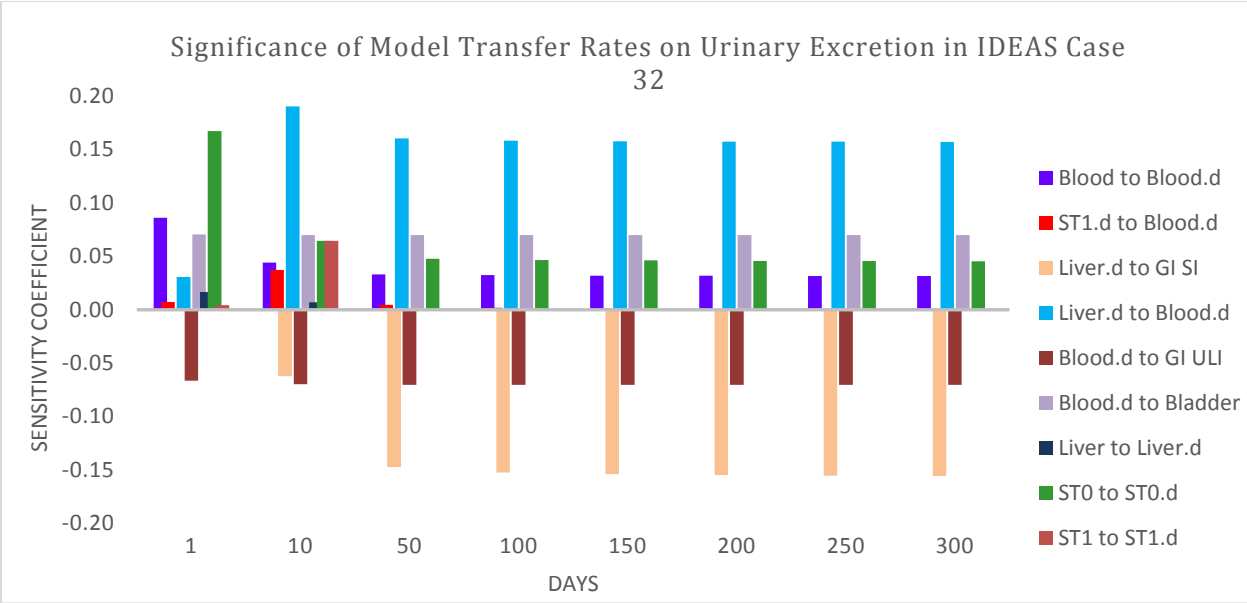


Fig. 4.5. Sensitivity coefficients for those complex transfer rates that have a significant influence on urinary excretion over a period of 300 days.

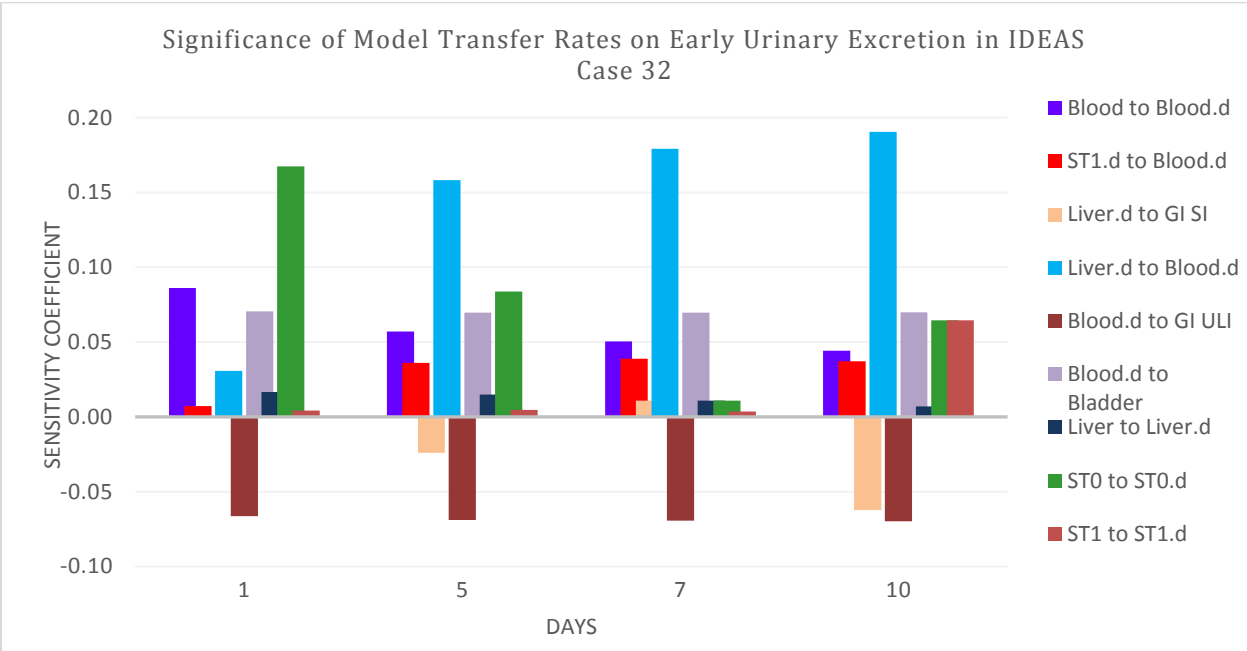


Fig. 4.6. Sensitivity coefficients for those complex transfer rates that have a significant influence on early urinary excretion in Case 32 following treatment days 1, 4, and 6.

The interpretation of this sensitivity analysis is that the most important pathways post Ca-DTPA treatment are the rapidly clearing soft tissues (ST0.d) and blood (Blood.d) pathways with

the liver pathways, Liver.d to Blood.d and Liver.d to GI ULI, dominating the prediction of urinary excretion after day 5.

This appears to imply that day 1 post-treatment, Ca-DTPA can effectively complex americium from the blood and rapidly clearing soft tissues and be rapidly excreted via the urinary pathway. This statement seems to agree with published data suggesting Ca-DTPA forms rapidly excreted complexes in the blood and soft tissues and accounts for the short biological half-time of Ca-DTPA. But the significance of these pathways becomes less important in the days following Ca-DTPA treatment, with the liver pathways to the blood and blood to upper large intestine becoming more influential on urinary excretion. This seems to suggest a soft tissue pool where Ca-DTPA can effectively complex americium and be rapidly excreted as well as the ability of Ca-DTPA to complex americium in the liver and be released to excretion at a slower rate.

4.3.2. Optimized Parameters

The transfer rates for the Liver.d to Blood.d and Liver.d to GI SI model pathways were initially optimized in an ad hoc manner, keeping in mind physiological significance, to find the most acceptable fit of the IDEAS Case 32 data. The data described in Table 10 represent the most acceptable fit of the data while remaining physiologically significant.

Table 10. Recommended transfer rates for the Am-DTPA compartmental model.

Compartment Pathway	Transfer Rate (d ⁻¹)	Compartment half-time	Compartment Pathway	Transfer Rate (d ⁻¹)	Compartment half-time
ST0 to ST0.d	3	332 min	Blood.d to ULI	4	250 min
ST1 to ST1.d	1.925	519 min	Blood.d to Bladder	25	40 min
Blood to Blood.d	1.378	724 min	Liver to Liver.d	0.9	0.8 days
ST0.d to Blood.d	99	10 min	Liver.d to Blood.d	0.015	46 days
ST1.d to Blood.d	0.1	7 days	Liver.d to SI	0.014	50 days
Blood.d to ST0.d	18	56 min			

The bolded transfer rates were all optimized from the suggested Pu-DTPA transfer rates. The data show increased retention of the Am-DTPA complex in the liver and intermediate soft tissues (ST1.d). The optimized model indicates the Am-DTPA complex is translocated from the Blood.d compartment with 53%, 38%, and 9% directed towards the Bladder, ST0.d, and GI ULI compartments, respectively. The model also accounts for the rapid exchange of DTPA between the ST0.d and Blood compartments with a half-time of 10 minutes.

The optimized model results in an IDEAS logarithmic chi-squared value of 102.24, with 75 degrees of freedom, and a p-value of 0.02. The autocorrelation statistic was calculated as 0.16, which was within the 95% confidence limit of 0.17. The maximum likelihood estimate of intake was calculated as 12,204 Bq. The optimized model compared to the Case 32 urine excretion is shown in Fig. 4.7. The *MLE.Lung* R function was used to perform these calculations and is shown in Appendix 1.

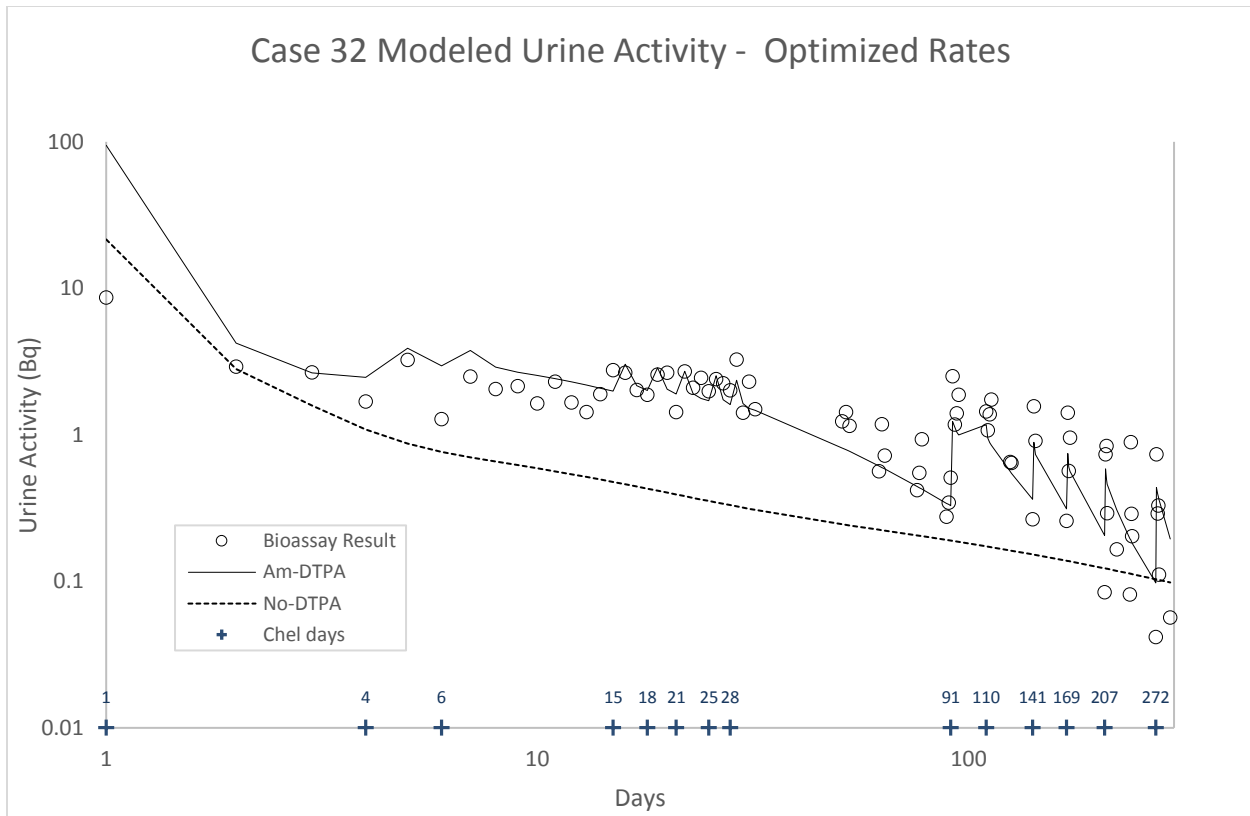


Fig. 4.7. Case 32 urine excretion compared to optimized model rates (solid line) with the dashed line representing the expected excretion for a 12.2 kBq intake without DTPA enhancement. The plus signs along the x-axis indicate a chelation day.

The optimized model data compared with the reference model transfer rates and suggested rates for the Am-DTPA complex are described in Table 11.

Table 11. Comparison of model statistics using Am-241 absorption type M for 5- μ m AMAD particles for Case 32 urine excretion.

	Reference Rates		Optimized Rates
	(No DTPA)	Pu-DTPA Rates	
MLE Intake (kBq)	44.6	12.9	12.2
χ^2	203.2	299.8	102.2
p-value	0	0	0.02
ρ	0.29	0.71	0.16
CV95	0.17	0.17	0.17

The autocorrelation results for the optimized transfer rates were within the 95% confidence limit, indicating acceptable performance of the urine bioassay prediction. However, the chi-squared value of the log-transformed data is just outside of the 95% confidence level. A

statistically significant chi-squared value for this data set is 96. The model is overestimating the urine excretion activity on day 1 by 77 Bq and underestimating the urine excretion activity on days 100 through 300 by an average of 0.2 Bq. The fit of the data must be rejected based on the criteria previously set for hypothesis testing, $p\text{-value} > 0.05$. However, the Am-DTPA model with the optimized parameters has an acceptable autocorrelation value at the 95% confidence limit, which may indicate bias in the assumed error (scattering factor) used to calculate the chi-squared value for these data. Therefore, the Am-DTPA transfer rates will be provisionally accepted to assess the fit of the USTUR Case 0846 urine data.

Lastly, the in-vivo skeletal measurements were compared to the model predictions as shown in Table 12 and Fig. 4.8. The retained activity in the skeleton was calculated using the *Am.Lung* function, which summed the activity in the cortical and trabecular bone surface and volume compartments for the respective measurement days. The activity was then scaled by the calculated geometric mean intake. The model prediction had a Pearson chi-square value of 0.69 and $p\text{-value}$ of 0.87 with 3 degrees of freedom, indicating a good fit of the skeletal activity.

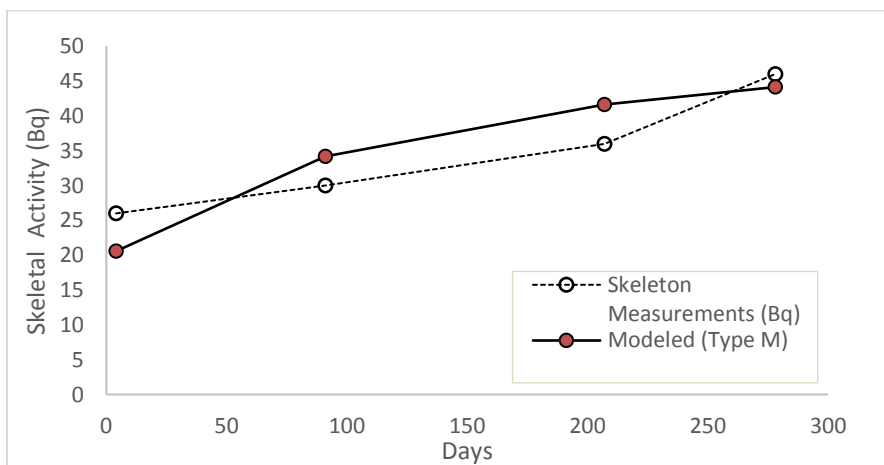


Fig. 4.8. Case 32 skeletal activity measurements compared to the Am-DTPA prediction of skeletal activity on measurement days.

Table 12. Case 32 skeleton activity measurements with predicted skeleton activity on measurement days.

Day	Skeleton Measurement (Bq)	Model Skeleton Activity (Bq)	Model IRF (Bq)	Est. Intake (Bq)
4	26	20.58	0.00660409	3937
91	30	34.17	0.01096694	2735
207	36	41.62	0.01335883	2695
278	46	44.14	0.01416603	3247
GEOMEAN Intake (Bq)				3116

4.4. USTUR Case 0846

The USTUR Case 0846 data set included extensive urine excretion measurements collected over a 7-year period. The subject was injected with a total of 322 grams of DTPA over a period of 337 weeks. The Ca-DTPA treatment strategies are summarized in Table 13. For the purposes of this report, period (a), which includes 460 consecutive daily urine measurements with weekly injections of 1-gram Ca-DTPA, will be assessed with the optimized Am-DTPA model.

Table 13. Ca-DTPA chelation treatment schedule divided into 9 contiguous periods starting in September 1967 (Rosen et al., 1980).

Period	Duration (wks)	Dose (g)	Frequency (doses/week)
a	65	1	1
b	2	0	--
c	14	0.5	2
d	31	0.5	1
e	37	1	1
f	19	0	--
g	56	1	1
h	22	0	--
i	134	1	1
Total	337	322	

The USTUR Case 0846 data set also included spot fecal samples during the first 80 weeks, and extensive radiochemical measurements made at autopsy. Assessments using these data sets are not in the scope of this report as the Am-DTPA model has been optimized for urine excretion but can be used for further analyses.

4.4.1. Model Assessment

As previously mentioned, Case 0846 involved an individual that prepared foils, produced in a compacting process, which contained up to 500 mCi of $^{241}\text{AmO}_2$ powder per foil. The initial exposure is presumed to have occurred in the first or beginning of the second year of work with the compaction process, placing the time of the exposure in 1965 or early 1965, although this is not certain (Rosen et. al., 1980). The individual performed this work for a period of 2 to 3 years, ending in May 1967, at which time he was removed from the work area. The individual began chelation therapy with weekly injections of Ca-DTPA in September 1967. This treatment regimen was continued for 65 weeks.

This case was modeled using two intake scenarios due to the uncertainty associated with the time of intake. (Scenario 1) assumes an acute intake one day prior to chelation therapy; and (Scenario 2) an acute intake of 1.2 MBq 379 days prior to beginning chelation therapy. The assumption in scenario 2 was proposed by Breustedt et al. (2012). Both scenarios are assuming an intake of 5- μm AMAD particles of Am-241 and evaluated using absorption types M and S.

Intake Scenario 1 Results

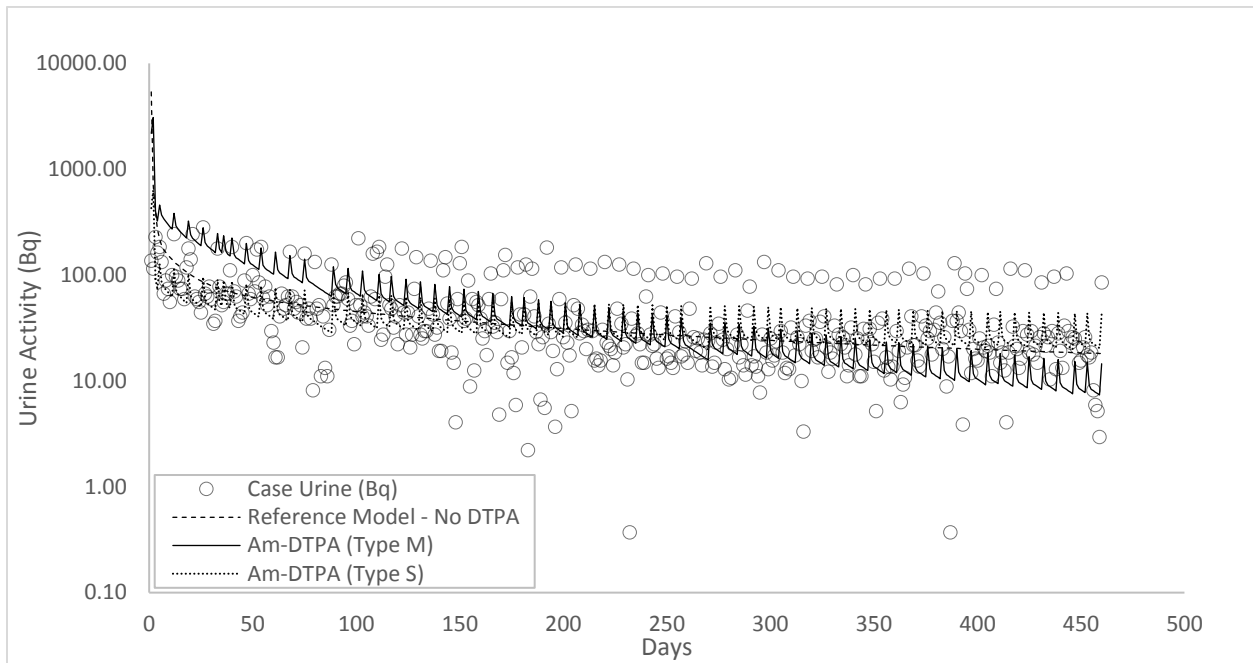


Fig. 4.9. Case 0846 urine excretion compared to reference model (No-DTPA) and the Am-DTPA model using Am-241 absorption types M and S

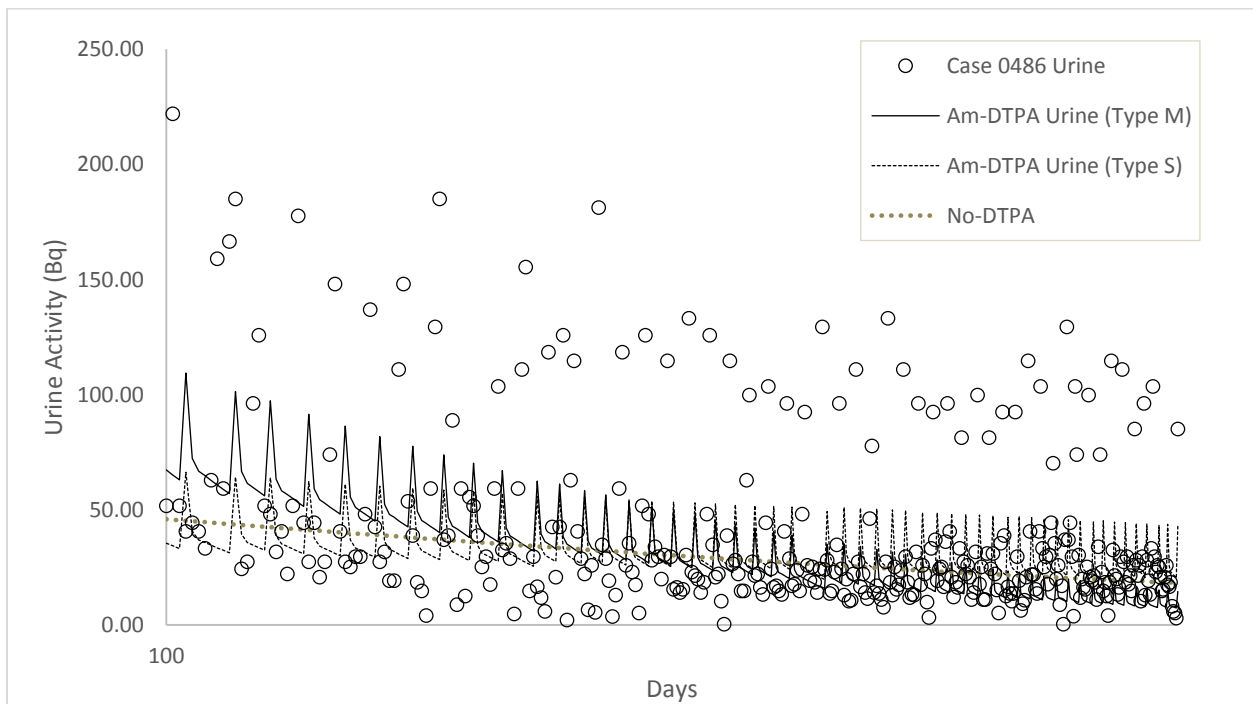


Fig. 4.10. Case 0846 urine excretion from day 100 to 460 compared to reference model (No-DTPA) and the Am-DTPA model using Am-241 absorption types M and S.

Table 14. Intake scenario 1 Case 0846 urine model statistics.

	Reference Rates (No DTPA)	Am-DTPA Rates (Type M)	Am-DTPA Rates (Type S)
MLE Intake (MBq)	3.04	1.23	24.03
χ^2	1429	2133	1560.4
Degrees of freedom	459	459	459
p-value	<0.05	<0.05	<0.05
ρ	0.20	0.43	0.22
CV95	0.07	0.07	0.07

Intake Scenario 2 Results

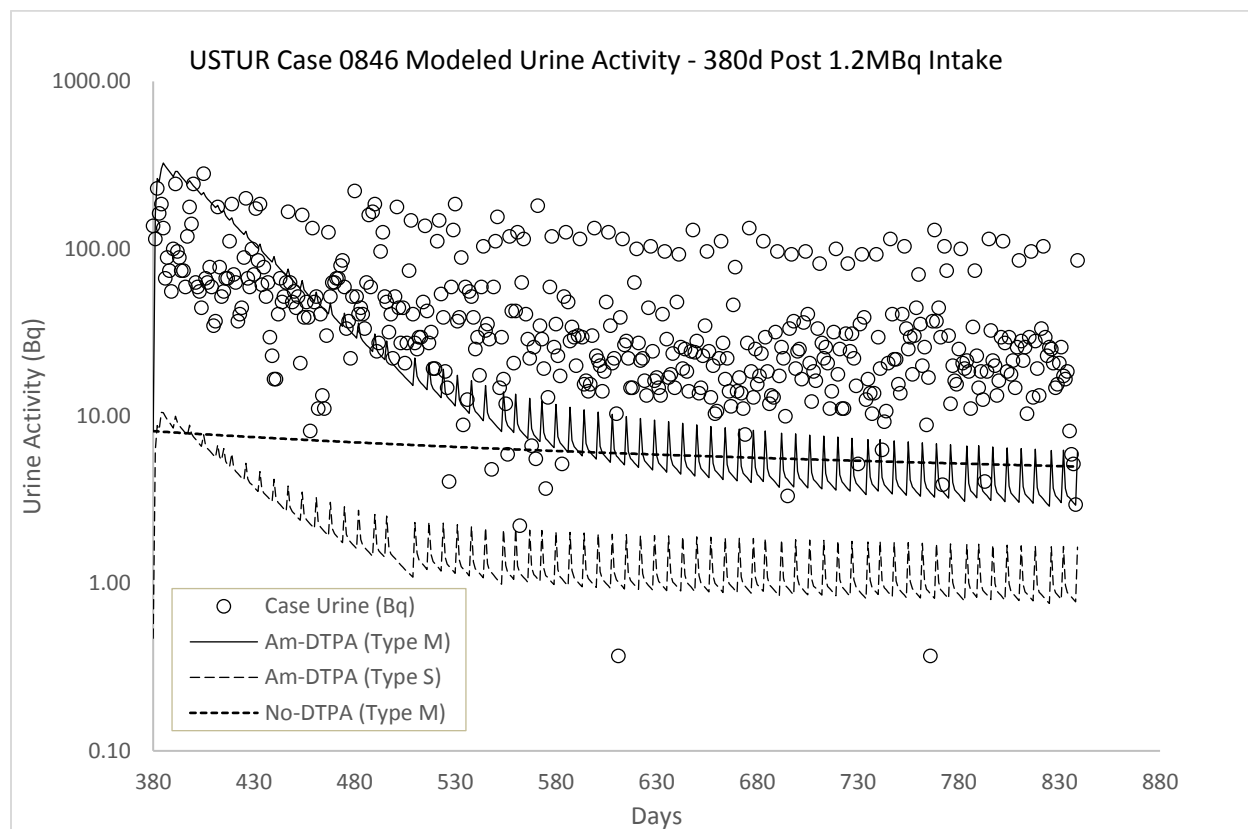


Fig. 4.11. Case 0846 urine excretion from day 380 to 840 compared to reference model (No-DTPA) and the Am-DTPA model using Am-241 absorption types M and S.

Table 15. Intake scenario 2 for Case 0846 urine model statistics.

	Reference Rates (No DTPA)	Am-DTPA Rates (Type M)	Am-DTPA Rates (Type S)
MLE Intake (MBq)	1.2	1.2	1.2
χ^2	7446	5419	21763
Degrees of freedom	459	459	459
p-value	<0.05	<0.05	<0.05
ρ	0.85	0.77	0.94
CV95	0.07	0.07	0.07

4.4.2. Case 0846 Summary

Neither intake scenario, modeled with the Am-DTPA model, was able to provide a good fit of the Case 0846 urine excretion data. The Am-DTPA model appears to be greatly underestimating the influence of chelation and excretion of Am-241 in this case and has not done well with understanding the peak of periodic excretion. However, the model did outperform the reference model in its ability to account for the increased excretion of activity post DTPA administration. Therefore, the model should be considered for future attempts at modeling chelation influenced data.

4.5. Hypothesis Testing

The following hypotheses were tested in this research:

H_{1,0}: The published Pu-DTPA transfer rates cannot be optimized for americium to adequately fit the Case 32 urine bioassay data

H_{1,A}: The published Pu-DTPA transfer rates can be optimized for americium to adequately fit the Case 32 urine bioassay data.

Test 1: The attempt to optimize the Pu-DTPA transfer rates to fit the Case 32 urine data resulted in a poor fit, accepting the null hypothesis.

The parameters set to evaluate the model were assessed using the chi-square and autocorrelation test statistics with a confidence level of $\alpha = 0.05$. Since these statistical tests were not in agreement at the 95% confidence level the model must be rejected. A model that has a good fit will have a p-value greater than the confidence level and a p value less than the respective autocorrelation confidence level.

H_{2,0}: The Am-DTPA transfer rates cannot be used to predict the published mean intake in IDEAS Case 32.

H_{2,A}: The Am-DTPA transfer rates can be used to predict the published mean intake in IDEAS Case 32

Test 2: The maximum likelihood estimate of intake was calculated as 12.2 kBq. An acceptable intake was taken to be within 10% of the published intake of 7.22 ± 1.69 kBq. Therefore, the null hypothesis must be accepted.

H_{3,0}: The Am-DTPA model using optimized Am-DTPA transfer rates cannot adequately fit the USTUR Case 0846 urine bioassay data

H_{3,A}: The Am-DTPA model using optimized Am-DTPA transfer rates can represent a good fit of the USTUR Case 0846 urine bioassay data

Test 3: The attempt to model the Case 0846 urine data was unsuccessful and greatly underestimated the excretion of Am-241. Modeling of Case 0846 urine data resulted in a poor fit and acceptance of the null hypothesis

5. Summary and Conclusion

5.1. Summary

The goal of this research was to estimate americium intakes from chelation influenced urine bioassay data using the published Pu-DTPA compartmental model coupled with current recommended biokinetic models. Transfer rates for the Am-DTPA were developed from a case study of IDEAS Case 32 and validation performed with USTUR Case 0846 urine data. The Am-DTPA model coupled with the ICRP reference models predicted an intake of 12.2 kBq in Case 32, while reference models alone estimated an intake of 44.6 kBq. The Am-DTPA model provided a better fit of the Case 32 urine data than reference models. Although, the intake estimation using the Am-DTPA model was not deemed statistically significant since the chi-square and autocorrelation value were not in agreement at the 95% confidence level. While not a statistically significant result, the Am-DTPA model resulted in an improved bioassay prediction, compared to reference models and suggested Pu-DTPA rates, when assessing chelation influenced urine bioassay data.

The validation of the Am-DTPA model using the first 65 weeks of DTPA influenced urine bioassay of USTUR Case 0846 proved to be inadequate. The Am-DTPA model provided a slightly better fit of the data than reference models using intake scenario 2. However, both models provide a poor fit of the data. A few contributing factors may include the great uncertainty associated with the time of intake and type of scenario (acute vs. chronic), the assumed particle size of 5- μm and absorption type M, the digitization of graphical data, and the length of DTPA treatment regimens may have altered the metabolism of americium in the body. Nevertheless,

the Am-DTPA model shows promise in its ability to model the rapid excretion of americium from the blood and soft tissues immediately following DTPA treatment.

5.2. Future Work

The Am-DTPA compartmental model shows promise in fitting chelation influenced urine data. The structure of the model appears to be physiologically significant in the biokinetic modeling of systemic americium and complexation with DTPA. Future research efforts may include further investigation of the rates of retention and removal of americium from the human liver, by DTPA, to the blood and biliary tract. These pathways appeared to dominate long-term excretion and retention of americium. Investigation into an additional pathway for urinary excretion, such as a kidney compartment, may assist in understanding the peak of periodic urine excretion in USTUR Case 0846. The transfer rates for the Am-DTPA complex may also provide a starting point for further optimization in other americium inhalation cases. The extension of the Am-DTPA model to injection, ingestion, and wound cases is also recommended.

6. References

- Ansoborlo E, Prat O, Moisy P, Den Auwer C, Guilbaud P, Carriere M, Gouget B, Duffield J, Doizi D, Vercouter T, Moulin C, Moulin V. Actinide speciation in relation to biological processes. *Biochimie* 88:1605-1618; 2006.
- Birchall A, James AC. A microcomputer algorithm for solving first-order compartmental models involving recycling. *Health Phys* 56:857-868; 1989.
- Breustedt B, Blanchardon E, Berard P, Fritsch P, Giussani A, Lopez MA, Luciani A, Nosske D, Piechowski J, Schimmelpfeng J, Serandour AL. The CONRAD approach to biokinetic modeling of DTPA decorporation therapy. *Health Phys*. 99(4):547-552; 2010.
- Breustedt B, McCord S, Tolmachev SY. Biokinetic modeling of chelation therapy for Am-241-USTUR Case 0846. 57th Annual Meeting of the Health Physics Society, Sacramento, CA, 22. - 26. July 2012, Abstract in: *Health Phys*:103(2) Supplement1; 2012.
- Breustedt B, Avtandilashvili M, McComish SL, Tolmachev SY. USTUR case 0846 – Modeling americium biokinetics after intensive decorporation. Proceedings of USTUR special session, 61st annual meeting of the Health Physics Society. Spokane: Health Physics Society; 2016.
- Brodsky A, Wald N. Experiences with early emergency response and rules of thumb. In: Brodsky A, Raymond H, Goans RE, Public protection from nuclear, chemical, and biological terrorism. Gaithersburg, MD: Health Physics Society; 2004: 335-371.
- Carbaugh EH, Lynch TP, Cannon CN, Lewis LL. Case study: three acute ²⁴¹Am inhalation exposures with DTPA therapy. *Health Phys*. 99(4):539-546; 2010.
- Castellani CM, Marsh JW, Hurtgen C, Blanchardon E, Berard P, Giussani A, Lopez MA. IDEAS guidelines (version 2) for estimation of committed doses from incorporation monitoring data. European Radiation Dosimetry Group (EURODOS) Report 01. Braunschweig; 2013.
- Chipperfield AR, Taylor DM. The binding of americium and plutonium to bone glycoproteins. *Eur. J Biochem*. 17:581-585; 1970.

Davesne E, Blanchardon E, Peleau B, Correze P, Bohand S, Franck D. Influence of DTPA treatment on internal dose estimates. *Health Phys* 110(6):551-557; 2016.

Durbin PW. Actinides in animals and man, pages 3339-3440. *The Chemistry of the Actinide and Transactinide Elements*, 3rd ed., Vol. 5, Morss LR, Edelstein NM, Fuger J. New York: Springer; 2006.

Fasiska BC, Bohning DE, Brodsky A, Horm J. Urinary excretion of ²⁴¹Am under DTPA therapy. *Health Phys*. 21:523-529; 1971.

Fritsch P, Grappin L, Guillermin AM, Fottorino R, Ruffin M, Miele A. Modelling of bioassay data from a Pu wound treated by repeated DTPA perfusions: biokinetics and dosimetric approaches. *Radiat. Prot Dosim* 127(1-4):120-124; 2007.

Gorden AE, Xu J, Raymond KN, Durbin P. Rational design of sequestering agents for plutonium and other actinides. *Chem. Rev.* 103:4207-4282; 2003.

Gremy O, Laurent D, Coudert S, Griffiths NM, Miccoli L. Decorporation of Pu/Am actinides by chelation therapy: new arguments in favor of an intracellular component of DTPA action. *Radiat Res.* 185:568-579; 2016.

Huckle JE, Sadgrove MP, Mumper RJ, Jay M. Species-dependent chelation of ²⁴¹Am by DTPA diethyl ester. *Health Phys.* 108(4):443-450; 2015.

International Atomic Energy Agency. Intercomparison and biokinetic model validation of radionuclide intake assessment. Vienna: IAEA; IAEA-TECDOC-1071; 1999.

International Commission on Radiological Protection. Limits on intake of radionuclides by workers. Oxford: Pergamon Press; ICRP Publication 30, Part 1; Ann ICRP 2(3/4); 1979.

International Commission on Radiological Protection. The metabolism of plutonium and related elements. Oxford: Pergamon Press; ICRP Publication 48; 1986.

International Commission on Radiological Protection. Limits on intake of radionuclides by workers: an addendum. Oxford: Pergamon Press; ICRP Publication 30, Part 4; Ann ICRP 19(4); 1988.

International Commission on Radiological Protection. Age-dependent doses to members of the public from intake of radionuclides: Part 2 Ingestion dose coefficients. Oxford: Pergamon Press; ICRP Publication 67; Ann ICRP 23(3/4); 1993.

International Commission on Radiological Protection. Human respiratory tract model for radiological protection. Oxford: Pergamon Press; ICRP Publication 66; Ann ICRP 24(1-3); 1994a.

International Commission on Radiological Protection. Dose coefficients for intakes of radionuclides by workers. Oxford: Pergamon Press; ICRP Publication 68; Ann ICRP 24(4); 1994b.

International Commission on Radiological Protection. Guide for the practical application of the ICRP human respiratory tract model. Oxford: Pergamon Press; ICRP Supporting Guidance 3; Ann ICRP 32(1-2); 2002.

International Commission on Radiological Protection. Human alimentary tract model for radiological protection. Oxford: Pergamon Press; ICRP Publication 100; Ann ICRP 36(1-2); 2006.

International Commission on Radiological Protection. Occupational intakes of radionuclides: Part 1. Oxford: Pergamon Press; ICRP Publication 130; Ann ICRP 44(2); 2006.

James AC, Sasser LB, Stuit DB, Glover SE, Carbaugh EH. USTUR whole body case 0269: demonstrating effectiveness of i.v. Ca-DTPA for Pu. Radiat. Prot Dosim 127(1-4):449-455; 2008.

Johnson TE, Birky BK. Health physics and radiological health, 4th ed. Lippincott Williams & Wilkins, Baltimore, MD; 2012.

Konzen K. Development of a plutonium-DTPA biokinetic model with suggested modification to the plutonium systemic model. Pocatello, ID: Idaho State University; 2014. Dissertation.

Konzen K, Brey R. Development of the plutonium-DTPA biokinetic model. Health Phys 108(6):565-573; 2015.

Konzen K, Brey R, Miller S. Plutonium-DTPA model application with USTUR case 0269. *Health Phys.* 110(1):59-65; 2016.

Khursheed A, Fell TP. Sensitivity analysis for the ICRP publication 67 biokinetic model for plutonium. *Radiat. Prot. Dosim.* 74(2):63-73; 1997.

Leggett RW. A retention-excretion model for americium in humans. *Health Phys.* 62(4):288-310; 1992.

Lindenbaum A, Rosenthal MW. Deposition patterns and toxicity of plutonium and americium in liver (invited paper). *Health Phys.* 22:597-605; 1972.

Menetrier F, Grappin L, Raynaud P, Courtay C, Wood R, Jousseineau S, List V, Stradling GN, Taylor DM, Berard PH, Morcillo MA, Rencova J. Treatment of accidental intakes of plutonium and americium: guidance notes. *Applied Radiation and Isotopes* 62: 829-846; 2005.

Menetrier F, Taylor DM, Comte A. The biokinetics and radiotoxicology of curium: a comparison with americium. *App. Radiat. Isot.* 66:632-647; 2008.

National Council on Radiation Protection and Measurements. Management of persons contaminated with radionuclides: scientific and technical bases. Bethesda, MD: NCRP; NCRP Report No. 161; 2008.

Paquet F, Ramounet R, Metivier H, Taylor DM. The bioinorganic chemistry of Np, Pu, and Am in mammalian liver. *J. Alloys Compounds*, 271-273: 85-88; 1998.

Rosen JC, Gur D, Pan SF, Wald N, Brodsky A. Long-term removal of ²⁴¹Am using Ca-DTPA. *Health Phys.* 39:601-609; 1980.

Slobodien MJ, Brodsky A, Ke CH, Horm I. Removal of zinc from humans by DTPA chelation therapy. *Health Phys.* 24:327-330; 1973.

Stricklin D, Rodriguez J, Millage KK, McClellan GE. Americium-241 decorporation model. A technical report sponsored by U.S. Defense Threat Reduction Agency, VA: DTRA-TR-15-2; 2014.

Sueda K, Sadgrove MP, Jay M, Di Pasqua AJ. Species-dependent effective concentration of DTPA in plasma for chelation of ²⁴¹Am. *Health Phys.* 105(2):208-214; 2013.

Stradling GN, Taylor DM, Kaul A, Becker D. Decorporation of radionuclides. Radiological protection. Braunschweig: Springer; 2005.

Taylor DM. The biodistribution and toxicity of plutonium, americium, and neptunium. *Sci. Total Environ* 83:217-225; 1989.

Taylor DM. The bioinorganic chemistry of actinides in blood. *J. Alloys Compounds*, 271-273; 1998.

Taylor DM, Stradling GN, Henge-Napoli MH. The scientific background to decorporation. *Radiat. Prot Dosim* 87(1):11-17; 2000.

Tortora GJ, Derrickson B. Principles of anatomy and physiology, 12th ed. New Jersey: John Wiley & Sons; 2009.

U.S. Department of Health and Human Services (DHHS). Toxicological profile for americium, Public Health Service Agency for Toxic Substances and Disease Registry, Atlanta GA; 2004.

U.S. Department of Energy (DOE). Selected radionuclides important to low-level radioactive waste management, National Low-Level Waste Management Program, Idaho Falls ID; 1996.

Volf V. Treatment of incorporated transuranium elements. International Atomic Energy Agency. Technical Report Series No. 184. Vienna; 1978.

Appendix 1: R Functions

The following R functions were used in this report were developed by Dr. Kevin Konzen for use in the Pu-DTPA biokinetic model. The R environment can solve exponential rate matrices by loading the *expm*⁴ package. The functions used in this research effort were developed by Konzen (2014) for the Pu-DTPA model but have been rewritten to describe the biokinetics of americium and the americium-DTPA complex. The functions were validated by comparing each respective output value to a published value to ensure agreement. The primary functions for this model are *decays*, *Am.lung.MLE*, *MLE.Lung*, and *sens*.

Decays

The *decays* function calculates the number of decays occurring in a compartment at any time provided the rate matrix [R], a decay time (t) and radioactive half-life (h) in days.

```
decays = function (R,t,h)
{
  X0=diag(as.matrix(R))
  lam=log(2)/h
  A=t(R)

  N = dim(R)[1]
  for (i in 1:N) {
    A[i, i] = -sum(R[i, -i]) - lam }

  A.exp=expm(A*t)
  B=A.exp-diag(1,dim(A)[1])
  trans=lam*solve(A) %*% B %*% X0
  X=A.exp %*% X0
  X[N-1]=X[N-1]+trans[N-1]
  X[N]=X[N]+trans[N]

  ttl = cbind(X0, X, trans)
  colnames(ttl) = c("initial", "atoms", "decays")
  row.names(ttl) = colnames(R)
  structure(list(summary = ttl), class = "decays") }
```

⁴ Vincent Goulet, Christophe Dutang, Martin Maechler, David Firth, Marina Shapira and Michael Stadelmann (2017). *expm*: Matrix Exponential, Log, 'etc'. R package version 0.999-2. <https://CRAN.R-project.org/package=expm>.

Decays Validation: Birchall and James I-131 Example

A validation of this function was performed using the example provided in Appendix C of Birchall and James (1989). The example involved calculating the number of β disintegrations in the thyroid 5000 days after the injection of 1 Bq of I-131 into the stomach compartment, using the ICRP metabolic model for iodine. Konzen (2014) also used this example to validate the decays function used in the Pu-DTPA model. Birchall (1989) concluded the number of β decays in the thyroid after 5000 days to be 2.675×10^5 . The decays function resulted in 2.659×10^5 β decays. The minor differences can be attributed to rounding errors.

```
I.decays = function(R,t,h)
#where R is rate matrix, t=decay time (d), h=halflife (d)
{
X0 = diag(as.matrix(R)) # setup initial quantity vector
lam = log(2)/h          # decay constant

A = t(R)                # A matrix created from R transpose
N = dim(R)[1]
for (i in 1:N) {
  A[i,i] = -sum(R[i,-i]) - lam
}
A.exp=expm(A*t)
B = A.exp - diag(1,dim(A)[1])
trans = lam*solve(A)%%B%%X0
X = A.exp %% X0
X[N-1] = X[N-1] + trans[N-1]
X[N] = X[N] + trans[N]

ttl = cbind(X0,X,trans)
colnames(ttl) = c("initial", "atoms", "decays")
row.names(ttl) = colnames(R)
structure(list(summary = ttl),class="decays")
}
```

```

> R=matrix(rep(c(0,0,0,0,0,0),6),nrow=6,byrow=TRUE)
> R[1,1]=1e6
> R[1,2]=24
> R[2,3]=0.3*log(2)/0.25
> R[2,5]=0.7*log(2)/0.25
> R[3,4]=log(2)/80
> R[4,2]=0.9*log(2)/12
> R[4,6]=0.1*log(2)/12
> row.names(R)=c("Stomach","Blood","Thyroid","Body","Urine","Feces")
> colnames(R)=c("Stomach","Blood","Thyroid","Body","Urine","Feces")
> R

```

	Stomach	Blood	Thyroid	Body	Urine	Feces
Stomach	1e+06	24.00000000	0.00000000	0.00000000	0.00000000	0.00000000
Blood	0e+00	0.00000000	0.8317766	0.00000000	1.940812	0.00000000
Thyroid	0e+00	0.00000000	0.00000000	0.00866434	0.00000000	0.00000000
Body	0e+00	0.05198604	0.00000000	0.00000000	0.00000000	0.005776227
Urine	0e+00	0.00000000	0.00000000	0.00000000	0.00000000	0.00000000
Feces	0e+00	0.00000000	0.00000000	0.00000000	0.00000000	0.00000000

```

> I.decays(R,5000,8.04)

```

	initial	atoms	decays
Stomach	1e+06	0.000000e+00	3579.323
Blood	0e+00	4.153739e-198	30339.956
Thyroid	0e+00	1.319421e-195	265988.092
Body	0e+00	2.210497e-196	16007.068
Urine	0e+00	6.830131e+05	683013.088
Feces	0e+00	1.072474e+03	1072.474

Am.Lung.MLE

This function was developed by Konzen (2014) to be coupled with the MLE.lung function but may also be used by itself. This function requires input of a rate matrix (R), the days when chelation was administered (d), time of interest (t), absorption type for Am-241 ("M" or "S"), and half-life (h). The resulting output is a table of intake retention fractions for the urine, faeces, blood, ST0, Lung, and ET compartments for the specified time of interest.

Example:

```
> Am.lung.MLE = function (R=R,d=c(1,4,6,15),t=20,type="M",h=432.2)
```

Function:

```
Am.lung.MLE= function (R=R,d=chel,t=10,type="M",h=432.2) {  
  #R is specified rate matrix that includes dtpa compartments  
  #d is days that chelation was applied  
  #type is absorption type "S" or "M" for Am  
  
  #ICRP 66 particle type "M" parameters  
  s.p=10; s.pt=90; s.t=0.005;  
  Lamb=0.0005  
  
  #ICRP 66 particle type "S" parameters  
  if(type=="S"){s.p=0.1; s.pt=100; s.t=0.0001; Lamb=0.00001;}  
  
  R[1:13,46]=s.p  
  R[15:27,46]=s.t  
  R[41,46]=Lamb  
  for(i in 1:13){R[i,14+i]=s.pt}  
  
  h.days = h * 365.25 #Am-241 half-life in days  
  
  R.dtpa=R  
  R.wo=R  
  R.wo[28:46,47:50]=0 #removes dtpa influence  
  
  Am.atoms = matrix(c(0, 0, 0, 0, 0, 0,0,0,0,0), nrow = 1, byrow = T)  
  colnames(Am.atoms) = c("Time(d)", "Urine", "Faeces", "Tot.Body",  
                        "Skeleton", "Liver", "Blood", "ST0", "lung", "ET")  
  Am.atoms = Am.atoms[-1, ]  
  df=1  
  N=(t/df)  
  
  for (i in 1:N) {  
    R=R.wo  
    for(j in 1:length(d)){  
      if(df<1){
```

```

        if(floor(i*df+1)==d[j]) R = R.dtpa}
    else {if(i==d[j]) R=R.dtpa} }

k = 1*df
n = i*df

last=decays(R,k,h.days)$summary[,2]
last1=last
last1[52:53]=0
if(k>=1) last1=decays(R,k-1,h.days)$summary[,2]

am.1 = last[53] - last1[53]
am.2 = last[52] - last1[52]
am.3 = sum(last[1:50])
am.4 = sum(last[33:38])
am.5 = sum(last[39],last[49])
am.6 = last[46]
am.7 = last[28]
am.8 = sum(last[1:10],last[15:24])
am.9 = sum(last[11:14],last[25:27])
am.new = matrix(c(n, am.1, am.2, am.3, am.4,
am.5,am.6,am.7,am.8,am.9), nrow = 1,
                byrow = T)
Am.atoms = rbind(Am.atoms, am.new)

#Update R matrix diagonal amounts based on last run
for(j in 1:length(last)){R.dtpa[j,j]=last[j];R.wo[j,j]=last[j];}
}
Am.atoms
structure(list(Am.atoms=Am.atoms))
}

```

Validation of the Am.lung.MLE function was performed through calculating the IRF values for inhalation of Am-241 5- μ m AMAD of type M and compared to those values published in IAEA Safety Report Series No. 37 (2004). The results are almost identical with minor errors that may be attributed to rounding as the IAEA table values are rounded to the tenth digit.

²⁴¹Am Inhalation (5- μ m AMAD, Type "M"):

\$Am. atoms	Time(d)	Urine	Faeces	Tot.Body	Lung	Skeleton	Liver	Blood
[1,]	1	1.780958e-03	1.162692e-01	0.48892640	5.745216e-02	0.007564533	0.012550675	1.591196e-04
[2,]	2	2.345382e-04	1.522948e-01	0.25733099	5.576690e-02	0.008313757	0.013770688	6.972625e-05
[3,]	3	1.318544e-04	7.715598e-02	0.15095621	5.482238e-02	0.008662118	0.014322957	3.548325e-05
[4,]	4	9.019614e-05	3.226006e-02	0.10790528	5.399460e-02	0.008856372	0.014618380	2.225965e-05
[5,]	5	7.204384e-05	1.280796e-02	0.09108850	5.319910e-02	0.008990825	0.014814000	1.708730e-05
[6,]	6	6.308722e-05	5.148472e-03	0.08442847	5.242403e-02	0.009101633	0.014970030	1.500490e-05
[7,]	7	5.783001e-05	2.238051e-03	0.08159950	5.166734e-02	0.009202683	0.015109595	1.411047e-05
[8,]	8	5.414868e-05	1.144166e-03	0.08020485	5.092831e-02	0.009299318	0.015241598	1.367421e-05
[9,]	9	5.121399e-05	7.304975e-04	0.07935070	5.020641e-02	0.009393606	0.015369486	1.341594e-05
[10,]	10	4.869460e-05	5.693178e-04	0.07870582	4.950114e-02	0.009486353	0.015494606	1.322804e-05
[11,]	20	3.319771e-05	3.659606e-04	0.07408721	4.326681e-02	0.010357941	0.016642347	1.190667e-05
[12,]	30	2.619672e-05	2.788837e-04	0.07063537	3.825872e-02	0.011146030	0.017634326	1.086054e-05
[13,]	40	2.254836e-05	2.140931e-04	0.06797531	3.418020e-02	0.011866003	0.018498805	1.000383e-05
[14,]	50	2.031771e-05	1.657014e-04	0.06589669	3.081175e-02	0.012529461	0.019257274	9.292239e-06
[15,]	60	1.874734e-05	1.294118e-04	0.06425079	2.799029e-02	0.013145346	0.019926415	8.692806e-06
[16,]	70	1.752698e-05	1.020792e-04	0.06293000	2.559419e-02	0.013720608	0.020519310	8.180910e-06
[17,]	80	1.651964e-05	8.139560e-05	0.06185535	2.353227e-02	0.014260714	0.021046342	7.738051e-06
[18,]	90	1.565797e-05	6.566294e-05	0.06096838	2.173587e-02	0.014770009	0.021515840	7.350255e-06
[19,]	100	1.490440e-05	5.362872e-05	0.06022555	2.015293e-02	0.015251990	0.021934577	7.006900e-06
[20,]	200	1.030314e-05	1.390600e-05	0.05630949	1.050989e-02	0.019018090	0.024221279	4.872440e-06
[21,]	300	7.966833e-06	7.418622e-06	0.05438403	5.808251e-03	0.021586094	0.024519555	3.776520e-06
[22,]	400	6.574199e-06	4.821241e-06	0.05304352	3.238056e-03	0.023464210	0.023874693	3.121432e-06
[23,]	500	5.683915e-06	3.416772e-06	0.05200645	1.809441e-03	0.024907705	0.022790030	2.701845e-06
[24,]	600	5.077616e-06	2.601437e-06	0.05115083	1.012672e-03	0.026061232	0.021529202	2.415550e-06
[25,]	700	4.637365e-06	2.108578e-06	0.05041078	5.675891e-04	0.027010087	0.020230537	2.207272e-06
[26,]	800	4.297751e-06	1.796482e-06	0.04974887	3.186125e-04	0.027806277	0.018964730	2.046332e-06
[27,]	900	4.021879e-06	1.587318e-06	0.04914330	1.791366e-04	0.028482813	0.017765805	1.915421e-06
[28,]	1000	3.788576e-06	1.438004e-06	0.04858092	1.008854e-04	0.029061685	0.016648000	1.804597e-06
[29,]	2000	2.424894e-06	8.127888e-07	0.04431125	3.591311e-07	0.031669137	0.009430890	1.155737e-06
[30,]	3000	1.788038e-06	5.670025e-07	0.04137692	1.562797e-09	0.031560220	0.006299132	8.524611e-07
[31,]	4000	1.433381e-06	4.401168e-07	0.03910750	8.023340e-12	0.030601914	0.004756210	6.835000e-07
[32,]	5000	1.208135e-06	3.643724e-07	0.03722744	4.553982e-14	0.029421670	0.003874803	5.761557e-07
[33,]	6000	1.050894e-06	3.136434e-07	0.03560493	2.718967e-16	0.028226224	0.003303221	5.012064e-07
[34,]	7000	9.343232e-07	2.769542e-07	0.03416756	1.662771e-18	0.027077964	0.002898150	4.456316e-07
[35,]	8000	8.445312e-07	2.491046e-07	0.03287046	1.029083e-20	0.025991008	0.002594517	4.028213e-07
[36,]	9000	7.734927e-07	2.272812e-07	0.03168336	6.413191e-23	0.024964322	0.002358570	3.689505e-07
[37,]	10000	7.160645e-07	2.097662e-07	0.03058469	4.016317e-25	0.023992885	0.002170411	3.415661e-07
[38,]	20000	4.390886e-07	1.272452e-07	0.02232210	4.558202e-47	0.016432992	0.001302727	2.094674e-07

IAEA Safety Report Series 37 Values:

Radionuclide: Am-241
 Intake: Inhalation Type M
 Aerosol size: 5.0 micron AMAD
 fl: 0.00050

Time (d)	Urine	Faeces	Tot. Body	Lungs	Skeleton	Liver
1	1.8E-03	1.1E-01	5.0E-01	5.8E-02	7.5E-03	1.3E-02
2	2.3E-04	1.5E-01	2.6E-01	5.6E-02	8.3E-03	1.4E-02
3	1.3E-04	8.0E-02	1.5E-01	5.5E-02	8.6E-03	1.4E-02
4	9.0E-05	3.3E-02	1.1E-01	5.4E-02	8.8E-03	1.5E-02
5	7.2E-05	1.3E-02	9.1E-02	5.3E-02	8.9E-03	1.5E-02
6	6.3E-05	5.3E-03	8.5E-02	5.3E-02	9.1E-03	1.5E-02
7	5.8E-05	2.3E-03	8.2E-02	5.2E-02	9.2E-03	1.5E-02
8	5.4E-05	1.2E-03	8.0E-02	5.1E-02	9.3E-03	1.5E-02
9	5.1E-05	7.4E-04	7.9E-02	5.0E-02	9.4E-03	1.5E-02
10	4.9E-05	5.7E-04	7.9E-02	5.0E-02	9.4E-03	1.5E-02
20	3.3E-05	3.7E-04	7.4E-02	4.3E-02	1.0E-02	1.7E-02
30	2.6E-05	2.8E-04	7.1E-02	3.8E-02	1.1E-02	1.8E-02
40	2.3E-05	2.1E-04	6.8E-02	3.4E-02	1.2E-02	1.8E-02
50	2.0E-05	1.7E-04	6.6E-02	3.1E-02	1.2E-02	1.9E-02
60	1.9E-05	1.3E-04	6.4E-02	2.8E-02	1.3E-02	2.0E-02
70	1.8E-05	1.0E-04	6.3E-02	2.6E-02	1.4E-02	2.0E-02
80	1.7E-05	8.2E-05	6.2E-02	2.4E-02	1.4E-02	2.1E-02
90	1.6E-05	6.6E-05	6.1E-02	2.2E-02	1.5E-02	2.1E-02
100	1.5E-05	5.4E-05	6.0E-02	2.0E-02	1.5E-02	2.2E-02
200	1.0E-05	1.4E-05	5.6E-02	1.1E-02	1.9E-02	2.4E-02
300	8.0E-06	7.4E-06	5.4E-02	5.8E-03	2.2E-02	2.4E-02
400	6.6E-06	4.8E-06	5.3E-02	3.3E-03	2.3E-02	2.4E-02
500	5.7E-06	3.4E-06	5.2E-02	1.8E-03	2.5E-02	2.3E-02
600	5.1E-06	2.6E-06	5.1E-02	1.0E-03	2.6E-02	2.2E-02
700	4.6E-06	2.1E-06	5.0E-02	5.7E-04	2.7E-02	2.0E-02
800	4.3E-06	1.8E-06	5.0E-02	3.2E-04	2.8E-02	1.9E-02
900	4.0E-06	1.6E-06	4.9E-02	1.8E-04	2.8E-02	1.8E-02
1000	3.8E-06	1.4E-06	4.9E-02	1.0E-04	2.9E-02	1.7E-02
2000	2.4E-06	8.1E-07	4.4E-02	3.6E-07	3.2E-02	9.4E-03
3000	1.8E-06	5.7E-07	4.1E-02	1.6E-09	3.2E-02	6.3E-03
4000	1.4E-06	4.4E-07	3.9E-02	8.1E-12	3.1E-02	4.8E-03
5000	1.2E-06	3.6E-07	3.7E-02	4.6E-14	2.9E-02	3.9E-03
6000	1.1E-06	3.1E-07	3.6E-02	2.7E-16	2.8E-02	3.3E-03
7000	9.4E-07	2.8E-07	3.4E-02	1.7E-18	2.7E-02	2.9E-03
8000	8.5E-07	2.5E-07	3.3E-02	1.0E-20	2.6E-02	2.6E-03
9000	7.7E-07	2.3E-07	3.2E-02	6.4E-23	2.5E-02	2.4E-03
10000	7.2E-07	2.1E-07	3.1E-02	4.0E-25	2.4E-02	2.2E-03
20000	4.4E-07	1.3E-07	2.2E-02	0.0E+00	1.6E-02	1.3E-03

MLE.Lung

Konzen (2014) states, MLE.Lung function analyzes inhalations with chelation, providing an estimated intake quantity accompanied with the standard statistics and plots with the actual bioassay sample results and the standard model prediction without chelation. The rate matrix is specified with incorporated ICRP 66 and ICRP 67 compartments, and with DTPA compartments specified. The chelation days are specified for 'd', and the time (t) that is the duration up to the specified period in days. This function accommodates particle solubility for 'type' and the particle's AMAD 'size'. The function will perform a comparison with the urine, fecal, blood, liver or lung bioassay measurements, which is specified by entering the bioassay type with the 'Exc' input criteria. The intake may be specified greater than 1 or set to 1 when the intake estimate is desired. The 'weight' refers to the chi-square goodness of fit indicator with either the 'model' prediction or 'actual' value listed in the denominator of the formula. The scattering factor is used for chi-squared statistic and since this function was developed for urine, the scattering factor is incorporated in the code as 1.6, and autocorrelation determination.

Example:

```
>MLE.Lung=function(R=Am.Lung,d=c(1,4,6,15),t=294,case=U32_00,type="M",size=5,Exc="urine",intake=1,title="",weight="model"){
```

Function:

```
MLE.Lung=function(R=R,d=chell,t=50,case=U32_00,type="M",size=5,Exc="urine",intake=1,title="",weight="model"){  
  
  # R is rate matrix that may or may not include the bound compartments, d  
  # is chelation days, t is time of interest  
  # case is excretion matrix of days and bioassay measurements  
  # type is the ICRP 66 absorption type (S,M of F)  
  # fb is the fraction going to the bound compartment in the ICRP 66 lung  
#model  
  # h is radioactive half-life in years  
  # intake may be specified or left as 1 for the function to determine  
  # title is used for the plot title  
  # weight is used in the denominator of for determining the chi-square  
#goodness of fit. Options are "actual" or
```

```

# "model", corresponding to either the actual data or the compartment
#model results.

N=case[dim(case)[1],1]
if(N<t)t=N else N=t

#truncated case when N>t
NN=dim(case)[1]
for(i in NN:1){
  if(case[i,1]>t)case=case[-i,]}

#determine whether Pu or Am by R matrix dimension
if(Exc=="urine")k=2
if(Exc=="fecal")k=3
if(Exc=="liver")k=6
if(Exc=="blood")k=7
if(Exc=="lung")k=9

X.s=Am.lung.MLE(R=R,d=d,t=t,type=type)$Am.atoms[,1:k];
X.z=Am.lung.MLE(R=R,d=0,t=t,type=type)$Am.atoms[,1:k];

X.s=cbind(X.s[,1],X.s[,k])
X.z=cbind(X.z[,1],X.z[,k])

X.o=X.s

#normalize results to case days for regression
for(i in N:1){
  rem=0
  for(j in 1:dim(case)[1]){
    if(X.s[i,1]==case[j,1])rem=1}
  if(rem==0)X.s=X.s[-i,]}

#specify intake to use
if(intake<=1){
  intake=exp(sum(log(case[,2]/X.s[,2])/dim(case)[1]))
}

X.U=X.s
X.U[,2]=intake*X.U[,2]
X.o[,2]=intake*X.o[,2]

#get final regression stats
res=case[,2]-X.U[,2]
if(weight=="actual") w=1/case[,2] else w=1/X.U[,2] #specify weight
vector
chi=t(res^2)%*%w

rsq=1-sum(res^2)/sum((case[,2]-ave(case[,2]))^2)
X.z[,2]=X.z[,2]*intake

#Chi.square calculated according to IDEAS Guidelines
IDEAS=sum((log(case[,2])-log(X.U[,2]))^2/(log(1.6)^2))

#determine autocorrelation statistic

```

```

Nu=dim(case)[1];
numU=0;
sResU=(log(case[,2])-log(X.U[,2]))/log(1.6)
denU=IDEAS
for(i in 1:(dim(case)[1]-1)){
  numU=((log(case[i,2])-log(X.U[i,2]))/log(1.6))*((log(case[i+1,2])-
log(X.U[i+1,2]))/log(1.6))+numU
}
acU=numU/denU

X=matrix(c(intake,chi,rsq,IDEAS,acU),nrow=1,byrow=T)
colnames(X)=c("Intake(Bq)","chi-Sq","rsq.U","IDEAS chisqr","acU")

X=matrix(c(intake,chi,rsq,IDEAS,acU),nrow=1,byrow=T)
colnames(X)=c("Intake(Bq)","chi-Sq","rsq.U","IDEAS chisqr","acU")

#plot results
low=min(X.o[,2])
low1=min(case[,2])
hi=max(X.o[,2])
hi1=max(case[,2])
if(low1<=low)low=low1
if(hi1>=hi)hi=hi1

plot(case,log="xy",ylim=c(low,hi),main=title,xlab="Days",ylab="Urine
Activity (Bq)")
lines(X.o,typ="l")
lines(X.z,typ="l",lty=3)
structure(list(X=X,Xs=X.s))
}

```

Sens

This function performs a sensitivity analysis over all the rate matrix specified compartments for the time periods of interest, while also segregating the most influential compartments for urine, feces, blood and skeleton. The input requires the rate matrix to be specified with the time period of interest (Konzen 2014).

Example: To find the important compartments for the 100th day for the R.Am rate matrix:

```
>sens(R=R.Am, t=100)
```

Function:

```
sens=function (R=R, t=1) {
  #the rate matrix must have urine in the last row and feces in the second
  #to last row
  #the rate matrix must have Cort.Surf and Trab.Surf as headers for the
  #bone surfaces

  val=matrix(c(0,0,0,0,0,0,0,0,0,0,0,0,0,0), nrow=1, byrow=T)
  colnames(val)=c("coef", "compartment.1", "compartment.2", "transfer.rate",
                  "row", "col", "U.sens", "F.sens", "B.sens", "BS.sens", "k1",
                  "k2", "k3")

  val=val[-1,]
  h.days=24110*365.25
  tf=50*365.25
  t=t
  N=dim(R) [1]
  for(i in 1:N){
    if(colnames(R) [i]=="Cort.Surf" || colnames(R) [i]=="CortBS" ||
colnames(R) [i]=="CortSurf")
      k1=i
    if(colnames(R) [i]=="Trab.Surf" || colnames(R) [i]=="TrabBS" ||
colnames(R) [i]=="TrabSurf")
      k2=i
    if(colnames(R) [i]=="Blood")
      k3=i
  }

  p=1
  for(i in 1:N){
    for(j in 1:N){
      if(R[i,j]>0 && i!=j) {
        u1=decays(R, t, h.days)$summary[N, 2];
        f1=decays(R, t, h.days)$summary[N-1, 2];
        s1=decays(R, tf, h.days)$summary[k1, 3] +
decays(R, tf, h.days)$summary[k2, 3];
        b1=decays(R, t, h.days)$summary[k3, 2];
        op=R[i, j];
      }
    }
  }
}
```

```

    dp=R[i,j]*1.01;
    R[i,j]=dp;
    u2=decays(R, t, h.days)$summary[N, 2];
    f2=decays(R, t, h.days)$summary[N-1, 2];
    s2=decays(R, tf, h.days)$summary[k1, 3] +
decays(R, tf, h.days)$summary[k2, 3];
    b2=decays(R, t, h.days)$summary[k3, 2];
    R[i,j]=op;
    su=round((u2-u1)/u1/0.01, digits=5);
    sf=round((f2-f1)/f1/0.01, digits=5);
    ss=round((s2-s1)/s1/0.01, digits=5);
    sb=round((b2-b1)/b1/0.01, digits=5);

val=rbind(val, matrix(c(p, row.names(R)[i], colnames(R)[j], R[i,j], i, j, su, sf,
                        sb, ss, k1, k2, k3), nrow=1, byrow=T));
    p=p+1; }
}
}
val=as.data.frame(val)
U.val=val[order(abs(as.numeric(as.matrix(val[, 7])))), decreasing=TRUE), ]
F.val=val[order(abs(as.numeric(as.matrix(val[, 8])))), decreasing=TRUE), ]
B.val=val[order(abs(as.numeric(as.matrix(val[, 9])))), decreasing=TRUE), ]
S.val=val[order(abs(as.numeric(as.matrix(val[, 10])))), decreasing=TRUE), ]

structure(list(val=val, U.val=U.val[1:10, ], F.val=F.val[1:10, ], B.val=B.val[1:10, ], S.val=S.val[1:10, ]))

}

```